

# RSC Advances



This is an *Accepted Manuscript*, which has been through the Royal Society of Chemistry peer review process and has been accepted for publication.

*Accepted Manuscripts* are published online shortly after acceptance, before technical editing, formatting and proof reading. Using this free service, authors can make their results available to the community, in citable form, before we publish the edited article. This *Accepted Manuscript* will be replaced by the edited, formatted and paginated article as soon as this is available.

You can find more information about *Accepted Manuscripts* in the [Information for Authors](#).

Please note that technical editing may introduce minor changes to the text and/or graphics, which may alter content. The journal's standard [Terms & Conditions](#) and the [Ethical guidelines](#) still apply. In no event shall the Royal Society of Chemistry be held responsible for any errors or omissions in this *Accepted Manuscript* or any consequences arising from the use of any information it contains.

1                   **Chemical Sensors and Biosensors for the Detection of Melamine**

2   Ying Li<sup>1</sup>, Jingyue Xu<sup>1</sup>, Chunyan Sun\*

3                   *Department of Food Quality and Safety, Jilin University, Changchun 130062, China*

4   **Abstract:** Melamine is an emerging contaminant in milk, infant formula and pet food.  
5   In order to increase the “false” apparent protein content in food products, melamine  
6   has been artificially and illegally used as non-protein nitrogen additive. This review  
7   focuses on chemical sensors and biosensors for detecting melamine residue. We  
8   present the principles, the mechanisms and the performances of the sensors including  
9   optical sensors, electrochemical sensors, aptamer-based sensors and immunosensors.  
10   We also propose the future perspectives in developing sensors for the detection of  
11   melamine.

12   **Keywords:** Food safety; Melamine; Chemical sensor; Biosensor; Optical sensor;  
13   Electrochemical sensor; Aptamer-based sensor; Immunosensor

14  
15  
16  
17  
18  
19  
20  
21  
22  
23  
24  
25  
26  
27

---

\*Corresponding authors. Tel.: +86 431 87836375; fax: +86 431 87836391 (C. Sun).

E-mail addresses: sunchuny@jlu.edu.cn; sunchunyan1977@163.com (C. Sun).

<sup>1</sup>First two authors contributed equally to this work.

28	<b>Contents</b>
29	1. Introduction
30	2. Chemical sensors for the analysis of melamine
31	2.1 Optical sensors
32	2.1.1 Colorimetric sensors
33	2.1.1.1 Gold nanoparticles-based sensors
34	2.1.1.2 Silver nanoparticles-based sensors
35	2.1.2 Fluorescence sensors
36	2.1.2.1 Dyes-based sensors
37	2.1.2.2 Quantum dots-based sensors
38	2.1.2.3 Metal nanoclusters-based sensors
39	2.1.2.4 Upconverting nanoparticles-based sensors
40	2.1.3 Chemiluminescence sensors
41	2.1.4 Others
42	2.2 Electrochemical sensors
43	2.2.1 Conversion of non-electroactive melamine into electroactive melamine complex
44	2.2.2 Application of electrochemical probes
45	2.2.3 Eлектроchemiluminescence sensors
46	2.2.4 Molecularly imprinted polymer-based sensors
47	2.2.5 Others
48	3. Biosensors for the analysis of melamine
49	3.1 Aptamer-based sensors
50	3.2 Immunosensors
51	3.2.1 Enzyme-linked immunosorbent assay (ELISA)
52	3.2.2 Immunochromatographic assay
53	3.2.3 Optical immunosensors
54	4. Perspective and conclusion
55	Acknowledgements
56	References
57	

## 58 1. Introduction

59 Melamine (1,3,5-triazine-2,4,6-triamine, or  $C_3H_6N_6$ ) contains a substantial  
60 amount of nitrogen which accounts for about 66% of its mass. It is commonly used in  
61 the production of melamine-formaldehyde polymer resins, which is a component in  
62 many plastics, adhesives, glues, fertilizer and laminated products, such as plywood,  
63 cement, cleansers and fire retardant paint.<sup>1,2</sup> However, the exposure to melamine may  
64 be particularly dangerous to human health. Melamine has low acute oral toxicity, but  
65 its high concentrations can induce renal pathology and even death in babies and  
66 children.<sup>3,4</sup> Melamine can be hydrolyzed to cyanuric acid *in vitro*. Cyanuric acid will  
67 in turn associate with melamine to form an insoluble melamine-cyanurate complex  
68 which may form stones in the urinary system, probably leading to acute renal failure  
69 by obstruction.<sup>5,6</sup> Besides, it will also cause a variety of renal toxic effects such as  
70 nephrolithiasis, chronic kidney inflammation and bladder carcinoma.<sup>7</sup>

71 In order to increase the “false” apparent protein content in food products,  
72 melamine has been artificially and illegally used as non-protein nitrogen additive. As  
73 a nitrogen-rich compound, it was adulterated in pet food and caused many deaths of  
74 cats and dogs in the United States and elsewhere.<sup>8</sup> The illness of pets firstly made  
75 people wonder that melamine ingestion might be very harmful to humans. A  
76 lamentable example of the toxic effects of melamine occurred in China in 2008. It has  
77 been reported that nearly 300,000 children ingested an infant formula adulterated with  
78 melamine, and at least six of them died.<sup>9</sup> After the initial reports of adulterated infant  
79 formula, melamine was found in many food items, especially in Chinese-sourced milk  
80 powder. Moreover, melamine was also detected in various imported items such as  
81 candies, beverages, and cookies.<sup>10</sup> The Chinese government promulgated an interim  
82 control limit for melamine at 1 mg/kg for infant formula and at 2.5 mg/kg for other  
83 milk products in October 2008, and this interim limit became official for all foodstuffs  
84 in April 2011.<sup>11</sup> The World Health Organization (WHO) has recommended the  
85 tolerable daily intake for melamine to be 0.2 mg/kg body weight per day, while, the  
86 US Food and Drug Administration (FDA) has updated the maximum residue levels of  
87 melamine in infant formula to be 1.0 mg/kg and 2.5 mg/kg for milk and other milk

88 products, respectively.<sup>12</sup>

89 It is vital to monitor and control the harmful effects of melamine. Thus, various  
90 analytical methods for the detection of melamine in feedstuffs and food products have  
91 been developed. Most of the published reports have discussed the detection of  
92 melamine using chromatographic techniques, such as high performance liquid  
93 chromatography (HPLC),<sup>13, 14</sup> ultra-performance liquid chromatography/tandem mass  
94 spectrometry (UPLC/MS/MS),<sup>15, 16</sup> and gas chromatography/mass spectrometry  
95 (GC/MS).<sup>17-19</sup> These instrumental methods are widely applied for melamine  
96 determination due to their great sensitivity and accuracy. However, they necessarily  
97 require various cumbersome sample preparation techniques and lack on-site  
98 applicability. More importantly, these methods based on chromatography and mass  
99 spectroscopy also require skilled personnel, have high operating costs, and are  
100 time-consuming.

101 As a kind of novel technique, sensors, especially chemical sensors and  
102 biosensors, have been developed rapidly and received considerable attention in recent  
103 years. Although a number of reviews about melamine determination in foodstuffs  
104 have been reported, the majority of them mainly focus on chromatographic  
105 techniques.<sup>20-22</sup> The discussion about sensing methods for scanning melamine is  
106 relatively rare. Hence, we comprehensively review the chemical sensors and  
107 biosensors for melamine detection developed in recent 5 years (Fig. 1).

## 108 **2. Chemical sensors for the analysis of melamine**

109 Chemical sensors are devices that transform chemical information, ranging from  
110 the concentration of a specific sample component to total composition analysis, into  
111 an analytically useful signal. Chemical sensors usually contain two basic components  
112 connected in series: a chemical (molecular) recognition system (receptor) and a  
113 physico-chemical transducer.<sup>23</sup> As chemical devices, they can react with different  
114 chemical components and have various applications, such as environmental and  
115 security monitoring, medical diagnosis, process control, pollution control and food  
116 analysis.<sup>24-27</sup> We discuss various chemical sensing methods developed for melamine  
117 in the following.

## 118 2.1 Optical sensors

119       Optical sensors recognized as analytical tools are of vital importance in the field  
120 of chemical sensors. By employing optical transduction techniques, they have been  
121 used to provide chemical information ranging from analyte concentration and binding  
122 kinetics to microscopic imaging and molecular structure. Based on photonic attributes  
123 of optical sensors, a variety of signal transduction pathways are utilized including  
124 absorbance, transmission, fluorescence intensity, chemiluminescence, refractive index,  
125 polarization, and reflectivity.<sup>28</sup> In the following sections, we discuss various optical  
126 sensors for melamine analysis including colorimetric sensors, fluorescence sensors,  
127 and chemiluminescence sensors.

### 128 2.1.1 Colorimetric sensors

129       Colorimetry, a kind of visual detection method, has drawn great attention due to  
130 its obvious advantages including simple instrument, easy operation, low cost while  
131 relatively high sensitivity. Localized surface plasmon resonance (LSPR) is one of the  
132 most obvious properties of metal nanoparticles (NPs) such as gold nanoparticles  
133 (AuNPs) and silver nanoparticles (AgNPs). LSPR of the metal NPs is primarily  
134 connected with the NPs size, shape, composition, interparticle distance, small or large  
135 aggregates of metal NPs, and dielectric constant (refractive index) of the surrounding  
136 medium. Especially, the decrease in the interparticle distance of NPs induced by the  
137 interaction between the analyte and NPs could result in a strong overlap between the  
138 plasmon fields of the nearby particles, which could cause a red-shift in the LSPR band  
139 with an increase in intensity and an easily observable color change.<sup>29</sup> On account of  
140 the excellent optical properties of noble metal NPs, especially of AuNPs and AgNPs,  
141 various colorimetric sensors employing functional metal NPs as colorimetric probes  
142 have been explored for the detection of a large of targets such as nucleic acids,  
143 proteins, saccharides, small molecules including melamine, metal ions, and even cells.

#### 144 2.1.1.1 AuNPs-based colorimetric sensors

145       Gold nanoparticles (AuNPs) own particular physical and chemical advantages  
146 such as simple synthesis process, unique and readily-tuned optoelectronic properties,  
147 excellent biocompatibility, high extinction coefficient, and good suitability for

148 multifunctionalization.<sup>30</sup> These unique properties make AuNPs excellent candidates  
149 for the fabrication of detection sensors. Particularly, the AuNPs-based colorimetric  
150 assays are of great interest because molecular recognition events can be easily  
151 transformed into color changes that arise from the interparticle plasmon coupling  
152 during AuNPs aggregation (red-to-purple or blue) or redispersion of an AuNPs  
153 aggregate (purple-to-red).<sup>31,32</sup>

154 With regard to melamine detection, the AuNPs-based colorimetric methods are  
155 certainly suitable owing to their simplicity and visibility. Based on the mechanism of  
156 color changes of AuNPs mentioned above, the reports of melamine detection could be  
157 classified into two types: AuNPs aggregation-based colorimetric sensors and AuNPs  
158 nonaggregation-based colorimetric sensors. One is owing to the aggregation of  
159 AuNPs, the other is in respect of the non-aggregation of AuNPs. The related assays  
160 are illustrated in Table 1.

161 In the AuNPs aggregation-based colorimetric sensors, two patterns have been  
162 utilized for the determination of melamine using unmodified AuNPs and  
163 ligand-functionalized AuNPs as colorimetric indicators. The first pattern employs the  
164 unmodified AuNPs as colorimetric probes which could be readily synthesized by the  
165 traditional Frens' method.<sup>33</sup> As illustrated in Fig. 2 A, the principle of this type of  
166 sensor is based on the fact that melamine can strongly bind with AuNPs through the  
167 interaction between amine groups of melamine and AuNPs, thus readily displace the  
168 stabilizing agents (citrate) from surfaces of AuNPs and cause the aggregation of  
169 AuNPs. Besides, the neighbour melamine-coated AuNPs could be cross-linked by  
170 NH $\cdots$ N hydrogen bonds between melamine molecules. For example, by conducting  
171 the control experiment with cyanuric acid, Li *et al.* have validated that only three  
172 amine groups of melamine are responsible for the cross-linking interaction between  
173 melamine and AuNPs which could induce the aggregation of AuNPs.<sup>34</sup> The sensitivity  
174 of two different nanometre-sized AuNPs (13 nm and 2.6 nm) was also studied,  
175 demonstrating a simple and rapid colorimetric method for melamine using a relatively  
176 more sensitive AuNPs with the particle size of 2.6 nm. The limit of detection for  
177 melamine is 0.4 part-per-million (ppm), and the whole process including sample

178 pretreatment takes only 12 min at room temperature. What's more, the method is  
179 specially promising for on-site rapid detection of melamine contamination in foods  
180 such as eggs and animal feeds. Similarly, Gao *et al.* reported a label-free  
181 AuNPs-based colorimetric kit for the detection of melamine employing 5 nm AuNPs  
182 which was more sensitive than 18 nm AuNPs verified in the assay.<sup>35</sup> The assay was  
183 performed by naked eye in comparison with the standard colorimetric card without  
184 the aid of any instrument. Determination of 1 ppm level was achieved by visual  
185 detection, and the method was suitable for rapid determination of melamine in most  
186 milk products, which could be used in the dairy industry, quality assurance  
187 departments, as well as by supermarket managers, customers *etc.* Guo and cooperators  
188 have developed a label-free AuNPs-based colorimetric method for the sensing of  
189 melamine using 13 nm AuNPs as the colorimetric indicator.<sup>36</sup> The sensing method for  
190 melamine in liquid milk and infant formula respectively demonstrated a detection  
191 limit of 1.0 and 4.2 ppm by naked eyes, while the detection limit of 0.15 and 2.5 ppm  
192 by UV-vis spectrometer. Zhang and cooperators have successfully explored a simple  
193 and effective colorimetric visualization of melamine in milk products employing 13  
194 nm citrate-stabilized AuNPs with the aid of NaHSO<sub>4</sub> optimization.<sup>37</sup> It has been  
195 demonstrated that the NaHSO<sub>4</sub>-optimized AuNPs system exhibits an excellent  
196 detection limit as low as ~25 parts-per-billion (ppb) on account that NaHSO<sub>4</sub> could  
197 promote the ligand exchange between citrate and melamine at the surface of AuNPs,  
198 thus promoting the aggregation of AuNPs. Recently, employing 8.1 nm  
199 dual-functional AuNPs with analyte-recognition and peroxidase-like activity, a facile  
200 method was proposed for the first time to sensitively detect melamine and highly  
201 improve the peroxidase-like activity of bare AuNPs at the same time.<sup>38</sup> Bare AuNPs  
202 have been demonstrated to possess intrinsic peroxidase-like activity. In this assay, the  
203 peroxidase-like activity of the AuNPs is evaluated by the catalysis of  
204 3,3',5,5'-tetramethylbenzidine (TMB) in the presence of H<sub>2</sub>O<sub>2</sub> to produce a blue color  
205 with a maximum absorbance at 652 nm. What's more, the study further revealed that  
206 the AuNPs-melamine aggregates formed after the addition of melamine can enhance  
207 the peroxidase-like activity of AuNPs to obtain a higher conversion of TMB to



208 oxidized TMB. Consequently, AuNPs-H<sub>2</sub>O<sub>2</sub>-TMB detection system for visual  
209 melamine determination has been established with the detection limit as low as 0.025  
210 ppb.

211 To stabilize the AuNPs and improve the sensitivity of the AuNPs-based  
212 colorimetric assay, it should be a potential choice to functionalize AuNPs with some  
213 suitable ligands. There have been some reports for melamine sensing using  
214 ligand-functionalized AuNPs as colorimetric recognition elements. As shown in Fig. 2  
215 B, the mechanism of this pattern usually relies on the unique interaction between  
216 ligand and melamine allowing the visual sensing of melamine. Lu *et al.* have  
217 developed a MTT-stabilized AuNPs-based colorimetric sensor for visual detection of  
218 melamine.<sup>39</sup> The first step was synthesis of a thiol-functionalized cyanuric acid  
219 derivative 1-(2-mercaptoethyl)-1,3,5-triazinane-2,4,6-trione (MTT). Then, the  
220 MTT-stabilized AuNPs (12 nm) was prepared by ligand-exchange reaction using MTT  
221 and citrate-stabilized AuNPs. As a result, they demonstrated initially that the color  
222 change of AuNPs (from red to blue) was induced by the triple hydrogen-bonding  
223 recognition between melamine and MTT, which resulted in excellent selectivity for  
224 detection of melamine in milk products with complicated components. Based on this  
225 principle, they obtained a detection limit of 2.5 ppb with visual detection within 1 min.  
226 In addition, these advantages substantially make this method quite promising for  
227 on-site and real-time detection of melamine in raw milk, infant formula, and other  
228 milk products. Liu *et al.* have described a very sensitive colorimetric method for  
229 melamine detection employing 3-mercapto-1-propanesulfonate (MPS) modified  
230 AuNPs as the probe.<sup>40</sup> The functional groups -NH<sub>2</sub> of melamine can interact with the  
231 sulfo group of MPS *via* strong hydrogen bonding which could induce the aggregation  
232 of the MPS-AuNPs, resulting in a dramatic color change from red to blue. Moreover,  
233 the sensitivity of the MPS-AuNPs system could be greatly improved by adding NaCl  
234 to the MPS-modified AuNPs solution which leads to a more rapid color change in the  
235 NaCl-optimized MPS-modified AuNPs system. Consequently, the melamine  
236 determination was achieved with the detection limit as low as 1.008 ppb. Xu and  
237 cooperators have synthesized 18-crown-6-thiol-modified AuNPs, and then established

238 a rapid, simple, selective and cost-effective colorimetric method for melamine  
239 determination based on the AuNPs aggregation induced by the formation of cavity  
240 complexes through the hydrogen bonds between the ether oxygen atoms of the  
241 18-crown-6-thiol and amine groups of melamine.<sup>41</sup> With an excellent detection limit  
242 of 6 ppb and a wide linear range from 10 to 500 ppb, the proposed method has the  
243 potential to sensitively and simply monitor melamine in common products. Using  
244 cysteamine-modified AuNPs and an effective sample pretreatment protocol, Zhang *et*  
245 *al.* have reported a sensitive assay for melamine in complex matrices.<sup>42</sup> In this assay,  
246 the modification of cysteamine onto citrate-stabilized AuNPs aimed to weaken the  
247 electrostatic repulsion force between the AuNPs so that a minute amount of melamine  
248 could induce the modified AuNPs to aggregate by hydrogen bonds between melamine  
249 and cysteamine. With the limit of detection at 1 ppm, the detection sensitivity of the  
250 method was about 100 times higher than that of the method using unmodified AuNPs.  
251 Melamine monitoring has been achieved through supramolecular assembly with  
252 riboflavin (R) *via* H-bonding in the platform of R stabilized gold nanoparticles  
253 (R-AuNPs), by colorimetric as well as UV-vis techniques.<sup>43</sup> In this assay, the ethylene  
254 glycol (EG) of the EG stabilized system was replaced by the stronger complexing  
255 agent riboflavin so as to form the stable riboflavin-capped AuNPs. Upon addition of  
256 melamine to R-AuNPs, R-melamine complexation occurs making the R-AuNPs less  
257 stabilized, causing their agglomeration. Based on the principle, the melamine  
258 detection was carried out. More importantly, the method is biocompatible as a result  
259 of the use of riboflavin (vitamin B<sub>2</sub>) and sensitive with a detection limit at 0.1 ppm.  
260 Raj *et al.* have described a highly sensitive analytical method based on AuNPs  
261 rationally tailored with recognition elements uracil-5-carboxylic acid (UCA) and  
262 2,4,6-trinitrobenzenesulfonic acid (TNBS) for the visual sensing of melamine at the  
263 ppb level.<sup>44</sup> The different interactions of melamine with these recognition elements  
264 induce a rapid visible color change of the tailored AuNPs from red to blue. Due to the  
265 aggregation of AuNPs, the results proved that the method employing TNBS-tailored  
266 AuNPs reporter based on the charge-transfer interactions is superior to UCA-tailored  
267 AuNPs reporter based on multipoint hydrogen-bonding interactions towards

268 melamine sensing. Guan and co-workers have reported a green colorimetric approach  
269 for sensing of melamine based on the aggregation of AuNPs stabilized with chitosan  
270 which was used as both reducing and stabilizing agent.<sup>45</sup> By controlling the  
271 concentration of chitosan, chitosan-stabilized AuNPs was prepared by 0.5% chitosan.  
272 In the aqueous solution, the as-prepared chitosan-stabilized AuNPs are stable due to  
273 the electrostatic repulsion of the negative capping agents, tripolyphosphate (TPP).  
274 However, upon the addition of melamine, the as-prepared chitosan-stabilized AuNPs  
275 could be aggregated induced by the electrostatic interaction between positively  
276 charged melamine and negatively charged chitosan-stabilized AuNPs, leading to a  
277 rapid, red-to-blue (dark blue or purple) color change. Based on the mechanism, the  
278 sensitive method for melamine sensing was established with a detection limit of 6 ppb.  
279 More importantly, the whole process could be accomplished within only 20 min  
280 including sample pretreatment allowing the rapid and sensitive detection of melamine.

281 Up to now, there are a few colorimetric assays for melamine by  
282 nonaggregation-based AuNPs as a probe, in which the synthesis of AuNPs was  
283 hindered or accelerated by the presence of melamine. Zhao and co-workers have  
284 developed a series of AuNPs nonaggregation-based colorimetric sensors realizing the  
285 melamine determination during the synthesis of AuNPs.<sup>46-48</sup> A simple colorimetric  
286 method for melamine monitoring employing nonaggregation-based AuNPs as the  
287 probe has been demonstrated.<sup>46</sup> In the assay, 3,5-dihydroxybenzoic acid (DBA) was  
288 used as a reducer for the reduction of Au<sup>3+</sup> ion to form AuNPs. In the absence of  
289 melamine, a one-step synthesis of AuNPs was achieved by mixing the Au<sup>3+</sup> ion with  
290 reducer DBA; in the presence of melamine, the formation of AuNPs was hindered by  
291 melamine because the strong hydrogen-binding interaction between melamine and  
292 DBA would make DBA not enough for the reduction of Au<sup>3+</sup>. Thus, the color change  
293 of formed AuNPs could be observed from purple to yellow-green with increasing  
294 melamine concentration, realizing the sensing of melamine during the formation of  
295 AuNPs with the detection limit of 1 ppb. Later, based on the similar principal that  
296 melamine could hinder the synthesis of AuNPs, this group reported a colorimetric  
297 detection of melamine based on the interruption of the synthesis of AuNPs using

298 ellagic acid (EA) as reducer.<sup>47</sup> The addition of melamine could make AuNPs change  
299 accompanied by color change from red to pale yellow. As a result, the melamine  
300 detection was carried out during the formation of AuNPs with the detection limit of  
301 0.2 ppb. Besides, relying on the different strategy that melamine could accelerated the  
302 formation of AuNPs, the group investigated a novel sensitive colorimetric method  
303 during the formation of AuNPs based on the principle that melamine could accelerate  
304 the synthesis of AuNPs.<sup>48</sup> In this study, the reducer 3,5-disodiumsulfonate (PD) may  
305 slow the synthesis of AuNPs in that PD can form intramolecular hydrogen-bonding in  
306 solution resulting in its weak reducing capacity. However, after the addition of  
307 melamine, the interaction of melamine with PD through hydrogen-bonding  
308 interrupted the intramolecular hydrogen-bonding of PD while promoted the reduction  
309 of Au<sup>3+</sup> by PD, resulting in the acceleration of the synthesis of AuNPs.  
310 Simultaneously, the melamine determination with a detection limit of 0.08 ppb could  
311 be realized *via* the color change of AuNPs from green to yellow in the process with  
312 the addition of different concentration melamine.

#### 313 2.1.1.2 Silver nanoparticles-based colorimetric sensors

314 Silver nanoparticles (AgNPs) have been proved to be effective catalytic materials  
315 for various applications owing to their large surface-to-volume ratio and electronic  
316 properties, and also exhibit higher extinction coefficients than AuNPs at the same  
317 size.<sup>49</sup> In the metal nanoparticle-based colorimetric assays, AgNPs have been used in  
318 less extension than AuNPs, however, a number of colorimetric methods have been  
319 established based on color change from yellow to brown during AgNPs dispersion and  
320 aggregation.<sup>29</sup>

321 Cai *et al.* have developed a reliable assay for melamine sensing using  
322 dopamine-stabilized AgNPs as a colorimetric reader.<sup>50</sup> Dopamine alone was used as  
323 both reducer to reduce Ag<sup>+</sup> and stabilizer to functionalize the generated AgNPs to  
324 synthesize monodispersed AgNPs with the color of bright yellow. However, upon the  
325 mixture of dopamine with melamine, the AgNPs aggregated and correspondingly the  
326 color changed from bright yellow to brown in that melamine could bind dopamine  
327 through Michael addition and Schiff base reactions. Consequently, the quantitative

328 monitoring of melamine was achieved at the 0.01 ppm level during the formation of  
329 AgNPs. Li *et al.* demonstrated a novel sensitive and low-cost colorimetric method  
330 using the stable  $\rho$ -nitroaniline-modified AgNPs, based on the melamine-induced  
331 aggregation and color change of AgNPs owing to electron donor-acceptor interaction  
332 between melamine and  $\rho$ -nitroaniline at the AgNPs interface.<sup>51</sup> Through the  
333 colorimetric response of AgNPs from yellow to blue, melamine detection was visually  
334 distinguished with the detection limit as low as 0.1 ppm. Ping and co-workers have  
335 established a visual detection method for melamine in raw milk employing label-free  
336 AgNPs as colorimetric probe, with the detection limit of 2.32  $\mu\text{M}$ .<sup>52</sup> The mechanism  
337 relies on the aggregation of AgNPs induced by the interaction between the three  
338 amino groups of melamine and AgNPs corresponding to the color change from yellow  
339 to red with the addition of different concentration of melamine. The proposed method  
340 with simplicity and rapidness is suitable for on-site screening melamine adulterant in  
341 milk products.

#### 342 2.1.2 Fluorescence sensors

343 Fluorescence sensors for targets detection have aroused great attention  
344 worldwide on account of their simplicity, high sensitivity, and easy operation.<sup>53</sup> This  
345 part mainly concentrates on the application of different fluorescent material as probes  
346 for melamine determination, including organic dyes, quantum dots, and metal  
347 nanoclusters *etc.*

##### 348 2.1.2.1 Dyes-based sensors

349 Fluorescence resonance energy transfer (FRET) is a nonradiative process  
350 whereby an excited state donor (usually a fluorophore such as dyes, quantum dots,  
351 *etc.*) transfers energy to a proximal ground state acceptor through long-range  
352 dipole–dipole interactions, and the rate of energy transfer is highly dependent on the  
353 extent of spectral overlap, the relative orientation of the transition dipoles, and  
354 especially the distance between the donor and acceptor molecules (typically in the  
355 range of 1-10 nm).<sup>54</sup> In the AuNPs-based FRET system, AuNPs can be used as  
356 excellent acceptors/quenchers due to their extraordinary advantages including high  
357 fluorescence quenching efficiency, tunable quenching property, stable optical property,

358 and ease of labeling.<sup>55</sup> In addition, the calculated energy-transfer distances are as long  
359 as 70-100 nm, about 10 times longer than the typical Förster distances ( $R_0$ ), as the  
360 distance dependence changes from  $R^{-6}$  to  $R^{-4}$ . So, using a gold metallic nanoparticle as  
361 an acceptor for energy transfer distinguishes nanomaterial surface energy transfer  
362 (NSET) from FRET in two significant aspects: (1) the distance dependent changes  
363 extends the usable distances for the measurement; (2) the same nanoparticle is able to  
364 quench dyes of different emission frequencies, spanning the visible range to the  
365 near-infrared.<sup>54</sup>

366 In recent years, the AuNPs-based FRET assays have been established for the  
367 analysis of small organic molecules including melamine which have affinity to bind  
368 on the AuNPs surface and could compete with dyes to adsorb onto gold surface. It has  
369 been reported that dyes (fluorescein, rhodamine B, *etc.*) could be adsorbed onto the  
370 surface of bare or functionalized AuNPs *via* electrostatic interaction, resulting in the  
371 significant fluorescence quenching through FRET between dyes and the AuNPs.  
372 While in the presence of targets, the fluorescence of dyes would recover owing to the  
373 competitive binding of dyes and analytes on AuNPs surface. Based on this principle  
374 (as illustrated in Fig. 3), Guo *et al.* have reported a novel sensitive turn-on  
375 FRET-based fluorescent sensor for melamine detection using fluorescein as donor and  
376 AuNPs as acceptor.<sup>56</sup> In this work, the fluorescence of fluorescein could be  
377 significantly quenched *via* FRET between fluorescein and the AuNPs. However, when  
378 melamine was incubated with AuNPs before fluorescein was added, the fluorescence  
379 was recovered as a result of AuNPs aggregation induced by the competitive  
380 interaction of AuNPs with melamine and fluorescein. Consequently, the rapid and  
381 sensitive detection of melamine was carried out within 15 min with the detection limit  
382 at 1 nM level. Relying on the similar strategy, employing rhodamine B (RB) as  
383 fluorescent probe accompanied with the AuNPs, an effective and practical method for  
384 melamine determination have been proposed based on the fluorescence quenching and  
385 recovery of RB through FRET and the competitive binding of RB and melamine on  
386 the AuNPs surface.<sup>57</sup> Consequently, the melamine detection was obtained with an  
387 excellent detection limit of 0.18 ppm. More importantly, through the fluorescence

388 recovery of RB linearly in proportion to melamine concentration, the melamine  
389 sensing in milk and powdered infant formula was successfully carried out with  
390 excellent recoveries varying from 95.9 % to 102.2 %. The proposed method appears  
391 to be a promising candidate method for rapid on-site screening of melamine  
392 contamination in dairy products.

#### 393 2.1.2.2 Quantum Dots-based sensors

394 Quantum dots (QDs), such as Cd-based QDs and Zn-based QDs, are  
395 nanocrystals made of semiconductor materials that are small enough to exhibit  
396 quantum mechanical properties. They possess unique optical properties including  
397 size-dependent excitation/emission spectrum, broad excitation spectrum and narrow  
398 emission spectrum, excellent photostability, good biocompatibility, high fluorescence  
399 quantum yields and long fluorescent lifetime. Owing to these superior properties, QDs  
400 have become ideal fluorescent probes for signal generation and transduction, and have  
401 been widely applied in the field of fluorescence sensing of analytes.<sup>58</sup>

402 A number of works for melamine monitoring directly employing QDs as  
403 fluorescent probes have been reported. The principle of this strategy is based on the  
404 enhancement and decrease of the fluorescence intensity of QDs induced by the  
405 interaction between QDs and target analytes. Our group has developed a simple and  
406 sensitive fluorescence sensor for melamine detection in milk using water-soluble  
407 thioglycolic acid (TGA)-CdTe QDs of different sizes.<sup>59</sup> Melamine could quench the  
408 fluorescence of TGA-CdTe QDs induced by the change of surface properties *via*  
409 hydrogen bonding between the amine groups of melamine and the carboxyl groups of  
410 the TGA-CdTe QDs at pH 8.0, which makes the proposed method used to detect  
411 melamine with a detection limit of 0.04 ppm. Later, Wang *et al.* have proved a  
412 sensitive and rapid method for melamine determination based on the fluorescence  
413 enhancement of TGA-CdS QDs.<sup>60</sup> At lower solution pH of 3.0, TGA-CdS QDs  
414 exhibited weaker fluorescence intensity in the absence of melamine. However, in the  
415 presence of melamine mixed with PBS before addition, the fluorescence intensity was  
416 enhanced in that the protonated TGA on the surface of QDs was replaced by the  
417 amine group of melamine which can attach onto the surface of QDs *via* N-Cd bond.

418 Through the increased fluorescence intensity with the increasing melamine  
419 concentration, the sensing of melamine was carried out with the detection limit of 1  
420 nM. Then, Zeng *et al.* have demonstrated an ultrasensitive sensing method for  
421 melamine using TGA-CdTe QDs based on the fluorescence intensity change of QDs  
422 through QDs aggregation at pH 11.0.<sup>61</sup> The pKa of carboxyl group in TGA is 3.53,<sup>62</sup>  
423 so the TGA-CdTe QDs are negatively charged in strong alkaline aqueous solution.  
424 Upon the addition of melamine, TGA on the surface of QDs could be replaced by  
425 melamine to form MA-coated CdTe QDs, consequently, the fluorescence of QDs  
426 were quenched with the surface change and aggregation of QDs induced by the  
427 electrostatic interaction between the negatively-charged TGA-CdTe QDs and  
428 positively-charged MA-coated CdTe QDs. Thus, the melamine detection was  
429 achieved according to the fluorescence intensity change of QDs. Most importantly,  
430 the proposed method possesses advantages of high sensitivity at  $5 \times 10^{-12}$  mol/L and  
431 good selectivity because the strong alkaline aqueous solution blocked interference  
432 from heavy metal ions in the samples. To improve the selectivity, a novel molecularly  
433 imprinted polymer-capped CdTe quantum dots (MIP-CdTe QDs)-based fluorescence  
434 detection method for melamine has been established relying on the fluorescence  
435 quenching of QDs induced by melamine.<sup>63</sup> The MIP-CdTe QDs were synthesized by  
436 a radical polymerization process among CdTe QDs, a template,  
437 3-aminopropyltriethoxysilane (APTES) and tetraethoxysilane (TEOS). Melamine  
438 could be selectively bound onto the surface of MIP-CdTe QDs resulting in the  
439 selective sensing of melamine with a detection limit of 0.6  $\mu$ M, hence, excellent  
440 selectivity and high sensitivity of MIP-CdTe QDs toward melamine were observed  
441 based on the fluorescence quenching of QDs.

442 Very recently, by combining QDs with graphene, Zhu *et al.* have reported a  
443 novel type of rapid and sensitive fluorescence sensing system for melamine using  
444 graphene quantum dots (GQDs) as fluorescence probes based on charge transfer  
445 quenching of the fluorescence of GQDs in the presence of  $\text{Hg}^{2+}$ .<sup>64</sup> In this study, the  
446 synthesized GQDs were strongly luminescent with predominantly aromatic  $\text{sp}^2$   
447 domains. Melamine could coordinate with  $\text{Hg}^{2+}$  through nitrogen atoms in both its



448 amine and triazine groups and bring more  $\text{Hg}^{2+}$  to the surface of GQDs through  $\pi$ - $\pi$   
449 stacking, thus leading to the fluorescence quenching of the of GQDs *via* charge  
450 transfer from the GQDs to  $\text{Hg}^{2+}$  with melamine acting as the linkage agent.  
451 Consequently, the melamine detection was carried out with a detection limit as low as  
452 0.12  $\mu\text{M}$ . The proposed method exhibits satisfactory advantages such as simple  
453 fabrication, convenient operation, high selectivity for melamine against interferences  
454 that may exist in real samples, and was suitable for detecting targets in real samples.

455 In addition to being directly recognized as fluorescent probes, QDs have also  
456 been used in donor-acceptor detection system based on the principle of FRET  
457 (mentioned in Section 2.1.2.1) or inner filter effect (IFE) of fluorescence. For example,  
458 Cao *et al.* have developed an efficient and enhanced FRET system between confined  
459 quantum dots (QDs) by entrapping CdTe QDs into the mesoporous silica shell  
460 ( $\text{CdTe@SiO}_2$ ) as donors and gold nanoparticles (AuNPs) as acceptors.<sup>65</sup> In this assay,  
461 compared with the energy transfer system between unconfined CdTe QDs and AuNPs,  
462 the fluorescence quenching efficiency of AuNPs to  $\text{CdTe@SiO}_2$  could be greatly  
463 improved in that AuNPs are noncovalently adsorbed on  $\text{CdTe@SiO}_2$  *via* an  
464 electrostatic interaction. In the absence of melamine, the  $\text{CdTe@SiO}_2$ -AuNPs  
465 assemblies coalesce to form larger clusters due to charge neutralization at pH 6.50,  
466 leading to the fluorescence quenching of  $\text{CdTe@SiO}_2$  as a result of energy transfer. In  
467 the presence of melamine, the weak fluorescence system of  $\text{CdTe@SiO}_2$ -AuNPs is  
468 enhanced due to the strong interactions between the amino group of melamine and the  
469 AuNPs *via* covalent bond, leading to the release of AuNPs from the surfaces of  
470  $\text{CdTe@SiO}_2$ . Relying on this strategy, the melamine determination was achieved with  
471 the detection limit of 0.89  $\mu\text{M}$ .

472 The mechanism of inner filter effect (IFE) of fluorescence refers to the  
473 absorption of the excitation and/or emission light of fluorophores by absorbers  
474 (quenchers) in the detection system.<sup>66</sup> IFE would occur effectively only if the  
475 absorption band of the absorber possesses a complementary overlap with the  
476 excitation and/or emission bands of the fluorophore. However, compared with  
477 QDs/AuNPs-based FRET systems, the design of IFE processes would be more

flexible and simple in that there is no need to modify AuNPs and QDs which aims to involve the intermolecular connection of QDs with AuNPs at a particular distance or geometry to enable the interaction between them. As a result, relying on the principle of IFE (as illustrated in Fig. 4), our group has explored a few IFE-based fluorescence assays for melamine determination in recent years. These assays can be classified into two types: AuNPs/Cd-based QDs IFE system, and AgNPs/Zn-based QDs IFE system. Based on IFE of AuNPs on the fluorescence of Cd-based QDs, two sensitive and rapid fluorescence methods for melamine sensing have been established employing CdTe QDs<sup>67</sup> and L-cysteine(L-Cys)-capped CdS QDs<sup>68</sup> as fluorescence probes respectively. In the assays, the obtained CdTe QDs and CdS QDs display a maximum fluorescence emission at 553 nm and 537 nm respectively, which is just near the absorption maximum of AuNPs at 522 nm. It is obvious that the absorption spectrum of AuNPs overlaps well with the fluorescence emission spectra of CdTe QDs and CdS QDs. Thus, the fluorescence of Cd-based QDs was obviously quenched upon addition of AuNPs *via* IFE. While with the presence different concentrations of melamine mixed and incubated with AuNPs before the addition of Cd-based QDs, the fluorescence of Cd-based QDs will gradually recover as a result of melamine-induced AuNPs aggregation. Consequently, the melamine detection was carried out with the detection limit at 0.02 ppm and 17 ppb level respectively. Recently, with eco-friendly L-glutathione-capped ZnSe QDs as fluorophore and citrate-stabilized AgNPs as absorber, a more practical and efficient fluorescence sensing strategy for melamine has been established for the first time based on the efficient IFE of AgNPs on the fluorescence of eco-friendly ZnSe QDs.<sup>69</sup> The emission spectrum of ZnSe QDs at 370 nm can overlap well with the absorption spectrum of AgNPs at 395 nm to some extent, suggesting that IFE might take place with ZnSe QDs as fluorophore and AgNPs as absorber. In the absence of melamine, AgNPs could effectively quench the fluorescence emission of ZnSe QDs through IFE. While in the presence of melamine, the fluorescence of QDs will recover due to the AgNPs aggregation induced by interaction between amine groups of melamine and AgNPs *via* hydrogen bonds. The IFE-based method has been successfully applied in melamine detection in raw milk

508 and egg samples with an excellent detection limit of 0.11 ppb.

### 509 2.1.2.3 Metal nanoclusters-based sensors

510 Metal nanoclusters (NCs), a new type of luminescent nanomaterials, are  
511 generally composed of a few to roughly a hundred atoms, and the sizes are below 2  
512 nm which approaches the Fermi wavelength of electrons, leading to the observation  
513 of dramatically different optical, electrical and chemical properties as compared to  
514 nanoparticles.<sup>70</sup> In recent years, metal NCs especially Au and Ag NCs have attracted a  
515 great deal of interest on account that they possess very strong, robust, size or  
516 scaffold-dependent tunable fluorescence, combine with good photostability and  
517 bio-compatibility, and show very high emission rates.<sup>71</sup> Due to these excellent  
518 features, Au and Ag NCs have been recognized as ideal fluorescent probes in the field  
519 of fluorescence sensing for melamine.

520 Xu *et al.* have successfully synthesized oligonucleotide-stabilized fluorescent  
521 silver nanoclusters (DNA-AgNCs) and applied them in melamine detection for the  
522 first time.<sup>72</sup> In the study, DNA-AgNCs could exhibit an emission band centered at 665  
523 nm when excited at 597 nm. In the presence of melamine, the fluorescence intensity  
524 of DNA-AgNCs could be gradually increased due to the microenvironment change of  
525 AgNCs induced by the interaction between the amine groups of melamine and  
526 thymine of DNA through strong hydrogen bonds. The proposed method demonstrated  
527 good biocompatibility and high sensitivity with the detection limit at 10 nM level.  
528 Recently, an environment-friendly and cost-effective turn-on fluorescent assay for  
529 melamine has been proposed employing bovine serum albumin stabilized gold  
530 nanoclusters (BSA-AuNCs) as the fluorescence probe.<sup>73</sup> It has been reported that the  
531 fluorescence of AuNCs could be quenched by Hg<sup>2+</sup> *via* high-affinity metallophilic  
532 Hg<sup>2+</sup> and Au<sup>+</sup> interactions.<sup>74</sup> Furthermore, melamine has been revealed greater  
533 coordination affinity toward Hg<sup>2+</sup>,<sup>75</sup> which may result in the reduction of quenching  
534 ability of Hg<sup>2+</sup> to AuNCs and accordingly the fluorescence enhancement of AuNCs.  
535 Based on the melamine-induced anti-quenching ability of Hg<sup>2+</sup> to fluorescent AuNCs,  
536 the method with the detection limit as low as 0.15  $\mu$ M was established and applied in  
537 real samples including raw milk and milk powder.

## 538 2.1.2.4 Upconverting Nanoparticles-based sensors

539 Upconverting (UC) nanoparticles are lanthanides ( $\text{Ln}^{3+}$ )-doped materials which  
540 are characterized by the conversion of long-wavelength radiation, for instance low  
541 energy infrared or near infrared (NIR) radiation, to short-wavelength high-energy  
542 radiation, usually in the visible range. UC nanoparticles exhibit high sensitivity  
543 because of the lack of autofluorescence background, possess less toxic components,  
544 and own high penetration depths in combination with photostability and optical  
545 tenability.<sup>76</sup> Owing to their outstanding properties, UC nanoparticles have been  
546 proposed for applications in chemical sensing,<sup>77</sup> bioconjugation and bioimaging,<sup>78</sup> *etc.*

547 Currently, hexagonal-structured lanthanide-doped  $\text{NaYF}_4$  has been reported the  
548 most promising candidate for detection. For example, Mahalingam *et al.* have  
549 reported for the first time the use of UC nanoparticles to detect melamine up to 2.5  
550 nM.<sup>79</sup> In this work, the water dispersible 3,5-dinitrobenzoic acid (DNB) capped  
551  $\text{NaYF}_4:\text{Yb}^{3+}/\text{Er}^{3+}$  nanocrystals were prepared by coating the surface of the  
552 nanocrystals with electron-deficient groups such as DNB through microwave  
553 procedure. Upon 980 nm excitation, the nanocrystals show strong upconversion  
554 emissions near 550 nm and 650 nm. Electron-rich melamine can be specifically  
555 attached onto the surface of the electron-deficient DNB-coated  $\text{Er}/\text{Yb}-\text{NaYF}_4$   
556 nanocrystals *via* strong charge transfer (CT) interaction (between amine groups of  
557 melamine and aromatic nucleus of DNB) and hydrogen bonding interaction (between  
558 O atom in  $-\text{NO}_2$  groups of DNB and H atom in  $-\text{NH}_2$  groups of melamine). Such  
559 interactions essentially decrease the interparticle distance between the nanocrystals  
560 and bring the nanocrystals close together resulting in the formation of aggregation.  
561 Hence, addition of melamine selectively quenches the luminescence signals from the  
562 upconverting nanocrystals because of the aggregation of the nanocrystals. The high  
563 selectivity toward melamine determination is verified by the addition of various  
564 analytes similar in structure with melamine. In addition, the selective quenching of the  
565 upconversion emission is found to be reversible by the addition of HCl, which  
566 recovered almost 90 % of the initial luminescence intensity. The high robustness,  
567 sharp emission peaks and large anti-Stokes shift make  $\text{Er}^{3+}/\text{Yb}^{3+}$ -doped  $\text{NaYF}_4$

568 nanocrystals a potential melamine sensing material over other organic fluorophores  
569 and nanocrystals.

### 570 2.1.3 Chemiluminescence (CL) sensors

571 Chemiluminescence (CL) refers to the phenomenon that the emission of light  
572 without incandescence due to a chemical reaction, in which a chemical species is  
573 excited to an electronically excited state and spontaneous generation of light occurs  
574 when it returns to its ground state.<sup>80</sup> It has low background scattering light  
575 interference and owns a variety of advantages such as high sensitivity, wide linear  
576 range, simple instrumentation, low cost, rapidity, safety and controllable emission  
577 rate.<sup>81</sup> CL can be measured using different device configurations, while the simplest  
578 dynamic CL instruments are based on a flow-injection (FI) analysis assembly where  
579 the reagents are discretely or continuously pumped into different streams and  
580 measured in-situ in the detection cell, leading to transient or continuous CL emissions,  
581 respectively.<sup>82</sup> When combined with FI manifold system, CL-detection acquires extra  
582 facilities, such as on-line sample processing and in-line multi-detector installment.<sup>83</sup>  
583 In addition, the CL process can take place *via* two strategies: one is the direct way  
584 through direct oxidation of the target analytes to produce emitting species, the other is  
585 the indirect way by means of exploiting the enhancing or inhibitory effects on the CL  
586 emission of certain luminescence compounds such as luminol, lucigenin, Ru(bpy)<sub>3</sub><sup>2+</sup>,  
587 or pyrogallol.<sup>84</sup> More interestingly, CL-based sensors have been recognized as one of  
588 the important techniques in the field of optical sensing for melamine.

589 Song *et al.* has explored a sensitive luminol-myoglobin CL system for the  
590 detection of melamine in milk products.<sup>85</sup> It was previously reported that myoglobin  
591 (Mb) could react with luminol in alkaline medium and yield strong CL emission.<sup>86</sup>  
592 While in the presence of melamine, the CL intensity generated from the luminol-Mb  
593 reaction would be hindered due to the interaction of melamine with Mb, resulting in  
594 the successful detection for melamine in milk products at 3 pg/mL level. Later, a  
595 simple and rapid flow injection chemiluminescence (FI-CL) method for the melamine  
596 sensing has been established using the luminal-H<sub>2</sub>O<sub>2</sub> system in which luminol was  
597 used as the CL reagent and H<sub>2</sub>O<sub>2</sub> as the oxidant.<sup>87</sup> Based on the principle that

598 melamine can significantly enhance the CL emission of the luminal-H<sub>2</sub>O<sub>2</sub> system in  
599 basic medium, the determination of melamine was achieved with the detection limit  
600 of 0.12 ppm. The proposed FI-CL method was suitable for high throughput and  
601 real-time melamine sensing on account of rapid detection time and excellent sample  
602 measurement frequency. Similarly, the luminal-H<sub>2</sub>O<sub>2</sub> system was also used in FI-CL  
603 method for melamine monitoring relying on the mechanism that melamine can  
604 accelerate the electrons transferring rate of excited 3-aminophthalate with notable  
605 enhanced CL intensity of luminol-H<sub>2</sub>O<sub>2</sub> reaction.<sup>88</sup> The low detection limit of 0.9 pg/  
606 mL and wide linear range from 2.5 to 250 pg/mL have demonstrated that the method  
607 was practical and could be applied in target analysis in complex samples. Another  
608 simple and sensitive FI-CL method for melamine determination has been developed  
609 based on the luminal-K<sub>3</sub>Fe(CN)<sub>6</sub> system.<sup>89</sup> A detection limit of 3.5 ng/mL could be  
610 achieved relying on the principal that melamine with different concentrations can  
611 gradually enhance CL signals from the luminal-K<sub>3</sub>Fe(CN)<sub>6</sub> system in an alkaline  
612 medium.

613 In addition, gold/silver alloy nanoparticles (Au/AgNPs) have been applied for  
614 melamine analysis in the field of CL-based sensors. For example, an ultrasensitive CL  
615 method has been developed for the determination of low concentrations of melamine  
616 employing permanganate-formaldehyde system (KMnO<sub>4</sub>-HCHO).<sup>90</sup> In the absence of  
617 Au/AgNPs, a weak CL could be observed in that KMnO<sub>4</sub> as CL reagent can oxidize  
618 HCHO. While in the presence of small volume of Au/AgNPs solution, the CL of  
619 KMnO<sub>4</sub>-HCHO could be obviously enhanced. However, upon the addition of  
620 melamine, the CL intensity of KMnO<sub>4</sub>-HCHO could be significantly decreased  
621 induced by melamine-coated NPs formed through the interaction between the three  
622 primary amine groups of melamine and NPs. Furthermore, the CL intensity was  
623 proportional to melamine concentration, realizing the determination of melamine with  
624 a detection limit of 8 pg/mL.

#### 625 2.1.4 Others

626 Conjugated polymers (CPs) have recently drawn worldwide attention as an  
627 effective optical transducer owing to their excellent signal amplification, convenient

628 optical detection, readily tunable properties, and easy fabrication.<sup>91</sup> As a result, a wide  
629 variety of conjugated polymers, including polythiophenes, polyanilines, polypyrroles,  
630 and polyphenylenes, as well as poly(phenylene ethynylenes), polyacetylenes, and  
631 polydiacetylenes have been investigated as sensing matrices. In the field of CPs-based  
632 sensors, polydiacetylene (PDA)-based chemosensors are unique in that they have the  
633 sensitive colorimetric/fluorescence dual detection capability and can be prepared  
634 through a simple molecular self-assembly followed by photopolymerization.<sup>92, 93</sup>  
635 Especially, a majority of PDA sensors involve the incorporation of specific receptors  
636 into the polymer or liposome. When a target molecule binds with the receptor, steric  
637 forces can change the PDA backbone conformation, resulting in the color change  
638 from blue to red. More interestingly, blue-phase PDAs is nonfluorescent, while its  
639 red-phase could exhibit fluorescence.<sup>94</sup>

640       Based on this strategy, Kim *et al.* have developed a rapid, sensitive, and selective  
641 PDA sensory system with dual signal capability for convenient melamine detection  
642 based on the multiple hydrogen bonding between cyanuric acid (CA) and melamine.<sup>95</sup>  
643 The PDA liposomes can be conveniently prepared by simple self-assembly and  
644 photopolymerization of rationally designed diacetylene molecules, composed of the  
645 mixture of 10, 12-pentacosadiynoic acid (PCDA) and the CA-carrying diacetylene  
646 monomer. Two types of CA-carrying monomers were synthesized and used, including  
647 PCDA-CA, and PCDA-EG-CA with the EG (ethyleneglycol) linker. It was  
648 demonstrated that the PDA liposomes of PCDA-EG-CA/PCDA was more sensitive to  
649 melamine and thus preferred on account that PCDA-EG-CA has the ethyleneglycol  
650 linker to match the length of its hydrophobic part with that of PCDA and also has a  
651 more balanced amphiphilic structure resulting in the production of intense blue color  
652 upon polymerization. The intra/inter liposomal hydrogen bonding between the target  
653 melamine and cyanuric acid receptor at the PDA liposome surface induces  
654 perturbation of the conjugated PDA backbone and results in rapid and sensitive  
655 colorimetric/fluorescence change of the PDA liposomes. The detection limit of the  
656 sensory PDA liposome is 1 and 0.5 ppm in the colorimetric and the fluorescence  
657 detection schemes, respectively, satisfying the world regulation level.

## 658 **2.2 Electrochemical sensors**

659 Electrochemical sensors are widely employed because of their instrumental  
660 simplicity, moderate cost and portability. They also provide many advantages such as  
661 good sensitivity and selectivity, remarkable rapidity and facility which are applicable  
662 to most areas of analytical chemistry.<sup>96</sup> A number of electrochemical strategies have  
663 been explored for the development of electrochemical sensors. Cyclic voltammetry  
664 (CV) has received great interest as it can be used for the elucidation of electrode  
665 processes and redox mechanisms. Differential pulse voltammetry (DPV) and square  
666 wave voltammetry (SWV) are particularly useful in the determination of trace  
667 amounts of electroactive compounds. Electrochemiluminescent (ECL) assays are also  
668 promising prospective technologies in that they combine the simplicity of  
669 electrochemistry with the inherent sensitivity and the wide linear range of the  
670 chemiluminescence method. Besides, electrochemical impedance spectroscopy (EIS)  
671 is a powerful tool for examining many chemical and physical processes in solution as  
672 well as in solids, and can provide information on reaction parameters, corrosion rates,  
673 electrode surfaces porosity, coating, mass transport, and interfacial capacitance  
674 measurements.

675 As a trimer of cyanamide with a 1,3,5-triazine skeleton, melamine has relatively  
676 poor electroactivity. Even though under strong alkaline conditions, it shows a very  
677 weak electrochemical response originating from the electrooxidation of the amino  
678 group. Thus, it's necessary to fabricate or utilize various electrochemical probes to  
679 realize the determination of melamine indirectly.

### 680 **2.2.1 Conversion of non-electroactive melamine into electroactive melamine** 681 **complex**

682 Electrochemical methods based on the redox properties of the analyte have been  
683 proved to be experimentally simple, and as such widely used for analytical  
684 applications. Unfortunately, the poor electrochemical property of melamine puts the  
685 direct voltammetric determination of melamine into a challenge. The first motivation  
686 for implementation of its electrochemical determination is to improve the  
687 electroactivity of melamine. Therefore, several indirect electrochemical methods for



688 melamine have developed by means of converting non-electroactive melamine into  
689 electroactive melamine complex.

690 Zhu and co-workers first explored a reliable and highly sensitive electrochemical  
691 sensor for the determination of melamine depending on that melamine could be  
692 converted to Cu-melamine complex with excellent electrochemical activity on the  
693 surface of a multi-walled carbon nanotubes-modified electrode by coordination of  
694 copper salt to melamine.<sup>97</sup> In this work, the Cu-melamine complex has been  
695 demonstrated to show a sensitive faradaic response, which makes it suitable for  
696 melamine detection as low as 0.25 ppb.

697 Later, based on an idea adopted from the synthesis of melamine formaldehyde  
698 resins, Liao *et al.* successfully developed a simple electrochemical strategy for  
699 sensitive and selective detection of melamine in dairy products and pet foods.<sup>98</sup>  
700 During a preconcentration step (at 1.8 V versus Ag/AgCl), melamine could interact  
701 with aldehyde to form a polymer at the preanodized screen-printed carbon electrode.  
702 The as-formed polymer was found to be electroactive with a reversible redox peak,  
703 and hence square-wave voltammetry was applied to further increase the detection  
704 sensitivity to meet the detection limit for application in real sample analysis. Simply  
705 with a medium exchange procedure, melamine was selectively detected with a  
706 detection limit (S/N = 3) of 0.8  $\mu\text{M}$  (*i.e.*, 98.3 ppb) by the square-wave voltammetry.  
707 The recovery tests established for external calibration and standard addition  
708 techniques verified that the analysis can be done in a single-run measurement. A  
709 single-run approach with the combination of disposable screen-printed carbon  
710 electrode and portable electrochemical instrument is actually suitable for on-site,  
711 real-time melamine testing.

### 712 **2.2.2 Application of electrochemical probes**

713 Considering the poor electrochemical activity of melamine, it is an excellent  
714 strategy to develop novel electrochemical sensors for melamine analysis by  
715 investigating the interaction between melamine and chemically modified electrodes  
716 with  $[\text{Fe}(\text{CN})_6]^{3-/4-}$  as the electrochemical indicator. Cao *et al.* first developed a  
717 surface electrochemical method for the determination of melamine in the milk

718 products based on oligonucleotides modified gold electrodes.<sup>99</sup> Oligonucleotides  
719 (d(T)20) containing a 6-mercaptohexyl linker at the 5' end was self-assembled onto  
720 the surface of gold electrode through the Au-S covalent interaction. The  
721 electrochemical probe of ferricyanide was used to investigate the interactions between  
722 oligonucleotides and melamine. Results of cyclic voltammeteries, differential pulse  
723 stripping voltammeteries, electrochemical impedance spectrometry and atomic force  
724 microscope, proved that melamine might interact with oligonucleotides mainly  
725 through electrostatic and hydrogen-bonding interactions. The interactions between  
726 oligonucleotides and melamine lead to the increase in the peak currents of  
727 ferricyanide, which could be used for electrochemical sensing of melamine. The  
728 redox peak currents of ferricyanide were linear with the concentration of melamine in  
729 the range from  $3.9 \times 10^{-8}$  to  $3.3 \times 10^{-6}$  M with the detection limit of  $9.6 \times 10^{-9}$  M.

730 Zhao *et al.* have explored a sensitive and environment-friendly electrochemical  
731 determination of melamine by DPV utilizing a glassy carbon (GC) electrode coated  
732 with the multi-wall carbon nanotube/chitosan (MWCNT/CS) composite.<sup>100</sup> A  
733 MWCNT/CS composite containing abundant groups (-OH, hydrogen bond) was  
734 prepared by electrostatic self-assembly with MWCNTs and CS.  $[\text{Fe}(\text{CN})_6]^{3-/4-}$  was  
735 used as the electrochemical probe to characterize the behaviors of the  
736 MWCNT/CS-modified GC electrode by CV and EIS. The modified GC electrode has  
737 a small electron-transfer resistance due to good conductivity of MWCNT, thus  
738 MWCNT/CS composite can greatly increase the conduction of electrons providing an  
739 improved electroanalytical response for ferricyanide ion. The interactions  
740 (electrostatic attraction and hydrogen-bonding interaction) between melamine and the  
741 MWCNT/CS composite could promote the electrochemical reaction of  $[\text{Fe}(\text{CN})_6]^{3-/4-}$   
742 at the MWCNT/CS modified GC electrode, suggested by the DPV of electrochemical  
743 probe  $[\text{Fe}(\text{CN})_6]^{3-/4-}$ . Thus, the melamine detection was achieved through the  
744 interaction between melamine and MWCNT/CS with the detection limit of 3 nM.  
745 Furthermore, this method can be directly applied to the determination of melamine in  
746 real milk, and did not need many complicated pretreatments such as centrifugation  
747 and filtration and the use of toxic solvent (*e.g.* trichloroacetic acid and methanol).

748 Up to now, in addition to ferricyanide used as the electroactive probe for facile  
749 voltammetric determination of melamine, melamine could also interact with some  
750 other electrochemical indicators and affect their electrochemical signals, which can  
751 therefore be used to build up novel electrochemical detection schemes. With  
752 3,4-dihydroxyphenylacetic acid (DOPAC) as the electrochemical probe and the  
753 recognition element, a new electrochemical sensor for melamine in milk products has  
754 been established at a glassy carbon electrode relying on the interaction between  
755 melamine and DOPAC.<sup>101</sup> Melamine has a good H-bonding ability and can  
756 spontaneously bind to the carboxyl group and two phenolic-OH groups of DOPAC to  
757 form a non-electroactive DOPAC-melamine complex.<sup>102</sup> The diffusion of the  
758 DOPAC-melamine complex is smaller than that of free DOPAC. Meanwhile, the  
759 hydrogen-bonding interaction restricts the electroactivity of the phenolic-OH group.  
760 Therefore, the redox peak currents of DOPAC decrease with the increasing  
761 concentrations of melamine. The anodic peak currents of DOPAC obtained by  
762 differential pulse voltammetry are linear with the logarithm of melamine  
763 concentrations in the range from  $1.0 \times 10^{-8}$  to  $5.0 \times 10^{-6}$  M with the detection limit of 3  
764 nM.

765 Liao *et al.* have successfully developed a simple and easy electrochemical  
766 approach for sensitive detection of non-electroactive melamine utilizing a disposable  
767 preanodized screen-printed carbon electrode (SPCE\*) with uric acid as the  
768 recognition element.<sup>103</sup> An improved electrochemical activity of uric acid was  
769 especially observed through the hydrogen bond between oxo-surface groups and the  
770 oxygen atom of the carbonyl group at C-2 in uric acid.<sup>104, 105</sup> The oxo-surface groups  
771 at the SPCE\* also provoke the adsorption of melamine that noticeably reduced the  
772 hydrogen bonding sites where uric acid reacted. Consequently, this assay is based on  
773 the competitive adsorption behavior of melamine at the SPCE\* causing suppression in  
774 the oxidation current of uric acid. A linear range up to 126 ppb with a detection limit  
775 of 1.6 ppb (S/N=3) is achieved at the SPCE\* by DPV. The established electrochemical  
776 method was successfully applied to detect the melamine content in tainted milk  
777 powder and dog food.

778 In addition to the hydrogen bonding recognition effect mentioned above, recently,  
779 the charge-transfer interaction between melamine and quinones has also been applied  
780 to develop a new voltammetric method for the determination of melamine at the  
781 glassy electrode.<sup>106</sup> For the three types of quinones employed, *i.e.*,  
782 tetrachloro-pbenzoquinone (TCBQ), benzoquinone (BQ), and vitamin K<sub>1</sub> (VK<sub>1</sub>),  
783 TCBQ exhibits the highest interaction activity with melamine due to its four  
784 electron-withdrawing chloro groups. Such a property was further employed for the  
785 voltammetric determination of melamine based on the decrease in the redox peak  
786 currents of TCBQ/TCBQ<sup>•-</sup> caused by the pre-consumption of TCBQ with melamine.  
787 Under the conditions employed in this study, the decrease in the peak current of  
788 TCBQ was linear with the concentration of melamine within a concentration range  
789 from 10 μM to 1.0 mM.

### 790 **2.2.3 Electrochemiluminescence sensors**

791 Electrochemiluminescence (ECL) involves the generation of species at electrode  
792 surfaces that undergo electron-transfer reactions to form excited states that emit light.  
793 Due to its advantages of high sensitivity and selectivity, wide linear range, good  
794 temporal and spatial control, versatility and simplified optical set up, ECL has  
795 received considerable attention for its wide use in pharmaceutical analysis,  
796 environmental monitoring, food safety, immunoassays, protein analysis and DNA  
797 diagnosis.<sup>107</sup> Among all the ECL systems, Ru(bpy)<sub>3</sub><sup>2+</sup>-based ECL is extensively  
798 studied for its high ECL efficiency and good stability in aqueous solution.<sup>108</sup>  
799 Compared with solution-phase ECL, solid-state ECL has several advantages, such as  
800 reducing the consumption of expensive ECL reagent Ru(bpy)<sub>3</sub><sup>2+</sup>, simplifying  
801 experimental design, and enhancing the ECL signal. Therefore, many efforts have  
802 been made to immobilize Ru(bpy)<sub>3</sub><sup>2+</sup> on the electrode surface to develop sensitive and  
803 selective solid-state ECL sensors. Considering the basic properties and also the three  
804 tertiary nitrogen atoms in its structure, melamine can be employed to be an amine  
805 additive reductant, to replace the tri-n-propylamine (TPA) in the commercially  
806 important Ru(bpy)<sub>3</sub><sup>2+</sup>-TPA ECL system.

807 An ECL enhancement method combined with solid-phase extraction has been

808 developed for the determination of melamine in dairy products.<sup>109</sup> The principle is  
809 that melamine could enhance the ECL of  $\text{Ru}(\text{bpy})_3^{2+}$  at glass carbon (GC) electrode in  
810 a strong base solution (pH=13). Melamine and  $\text{Ru}(\text{bpy})_3^{2+}$  could be oxidized on the  
811 electrode, and the active neutral free radical intermediate produced by the oxidation of  
812 melamine would react with the electrogenerated  $\text{Ru}(\text{bpy})_3^{3+}$ . As a result, the excited  
813  $\text{Ru}(\text{bpy})_3^{2+*}$  would be produced, which leads to the strong enhancement of the ECL  
814 signal. The enhanced ECL intensity was linearly proportional to the logarithm of  
815 melamine concentration with the detection limit of 0.003 ppb.

816 Liu *et al.* have studied the ECL of  $\text{Ru}(\text{bpy})_3^{2+}$  in the pH=10 borate buffer at the  
817 bare GC electrode and the single-wall carbon nanotubes (SWNTs) modified GC  
818 electrode for the determination of melamine.<sup>110</sup> It was confirmed that melamine can  
819 be a candidate as an amine co-reactant and react with  $\text{Ru}(\text{bpy})_3^{2+}$  instead of TPA. In  
820 addition, the planar electron-rich melamine molecule can be stacked on the surface of  
821 SWNTs through strong  $\pi$ - $\pi$  interaction. Notably, it was found that after addition of  
822 melamine, some increasing effect on both the ECL and anodic current intensity at  
823 SWNTs-modified GC electrode can be observed in comparison with that at bare GC  
824 electrode, owing to the collection and enrichment function of the SWNTs. Thus, the  
825 simultaneous immobilization of  $\text{Ru}(\text{bpy})_3^{2+}$  and melamine on the surface of the  
826 SWNTs provides a possibility to alter the interaction between the  $\text{Ru}(\text{bpy})_3^{2+}$  and  
827 melamine reductant from intermolecular to something like 'both intra- and  
828 inter-molecular' on the electrode surface. Furthermore, due to the increased effective  
829 area of the electrode, the electron transfer reaction on the SWNTs surfaces would be  
830 promoted. As a result, the ECL could be increased significantly. The detection limit  
831 for melamine can be reduced from  $1.0 \times 10^{-10}$  M at the bare GC electrode to  $1.0 \times 10^{-13}$   
832 M after modification of the GC electrodes by SWNTs.

833 A novel ECL approach for the melamine monitoring has been established by  
834 immobilizing  $\text{Ru}(\text{bpy})_3^{2+}$  onto the electrode surface.<sup>111</sup> The  $\text{Ru}(\text{bpy})_3^{2+}$  was first  
835 loaded into the sulfhydryl modified MCM-41 mesoporous silica nanoparticles (MSN)  
836 through the electrostatic absorption. Then the  $\text{Ru}(\text{bpy})_3^{2+}$ -doped MSN was  
837 immobilized onto the surface of Au electrode by Au-S interaction. As mentioned

838 above, melamine could replace the TPA in the  $\text{Ru}(\text{bpy})_3^{2+}/\text{TPA}$  ECL system and then  
839 realize the detection of melamine. The proposed solid-state ECL sensor provides a  
840 new strategy possessing the advantages of simplicity and low cost. Compared with the  
841 solution-phase  $\text{Ru}(\text{bpy})_3^{2+}$  ECL system, it will reduce the consumption of expensive  
842 reagent and simplify the experimental design. Particularly, it is a regenerable sensor  
843 based on  $\text{Ru}(\text{bpy})_3^{2+}$  recycled at the electrode surface during the ECL reaction.

844 Jia *et al.* also developed a solid-state ECL sensor for melamine based on  
845 mesoporous  $\text{SiO}_2/\text{Ru}(\text{bpy})_3^{2+}/\text{Nafion}$  modified GC electrodes.<sup>112</sup> The homogeneous  
846 mesoporous silica nanospheres were synthesized using modified Stöber sol-gel  
847 process. Since Nafion was known to contain a hydrophobic domain or phase  
848 composed of fluorocarbon skeleton, a hydrophobic cation  $\text{Ru}(\text{bpy})_3^{2+}$  can be easily  
849 incorporated into the composite films composed of cation-exchangeable Nafion and  
850  $\text{mSiO}_2$  nanospheres *via* both an ion-exchange process and hydrophobic interactions.  
851 The ECL and electrochemistry of the modified electrodes were investigated in detail  
852 with TPA as the coreactant. In the presence of TPA, the oxidation current increases but  
853 the reduction current decreases, at the same time, the enhanced ECL signal was  
854 observed, which was consistent with the  $\text{Ru}(\text{bpy})_3^{2+}$ -TPA reaction mechanism.<sup>107</sup> The  
855 modified electrodes were applied in testing melamine because of the similar structure  
856 of TPA and melamine. Furthermore, it has been successfully applied to determine  
857 melamine in milk powder. The proposed detection method has shown advantages  
858 including high sensitivity, stability and wide linear range, resulting from the high  
859 surface area and special structure of the mesoporous silica nanospheres for loading  
860  $\text{Ru}(\text{bpy})_3^{2+}$  species.

861 Similarly, another ECL sensor for melamine based on  $\text{Ru}(\text{bpy})_3^{2+}$ -doped silica  
862 ( $\text{Ru}(\text{bpy})_3^{2+}@\text{SiO}_2$ ) nanoparticles and graphene composite has been fabricated  
863 recently.<sup>113</sup> Spherical  $\text{Ru}(\text{bpy})_3^{2+}@\text{SiO}_2$  nanoparticles with uniform size about 55 nm  
864 were prepared by the reverse microemulsion method. An emerging carbon material,  
865 graphene, was adopted to improve the conductivity, resulting in greatly enhanced ECL  
866 signal. Due to its extraordinary electric conductivity, graphene improved the  
867 conductivity and accelerated the electron transfer rate. In addition, graphene could

868 work as electronic channel improving the efficient luminophor amount participating  
869 in the ECL reaction, which further enhanced the ECL signal. Combined with the high  
870 Ru(bpy)<sub>3</sub><sup>2+</sup> loading capacity of Ru(bpy)<sub>3</sub><sup>2+</sup>@SiO<sub>2</sub> nanoparticles and the high  
871 conductivity of graphene, the developed solid-state ECL sensor exhibited excellent  
872 performance and high sensitivity for melamine detection with a detect limit as low as  
873  $1 \times 10^{-13}$  M.

#### 874 **2.2.4 Molecularly imprinted polymer-based sensors**

875 Molecularly imprinted polymer (MIP), which is synthesized through the  
876 molecular imprinting techniques, possesses the advantages of specific recognition and  
877 selective adsorption of the target molecule (template molecule) and its structural  
878 analogs. Owing to the excellent advantages of high thermal stability, easy preparation,  
879 great reusability, predictable specific recognition and favorable selectivity, MIP has  
880 been extensively utilized as recognition elements and combined with electrochemical  
881 sensors to improve the selectivity of the sensors.<sup>114, 115</sup> The principal of these sensors  
882 mainly rely on electrochemical signal changes induced by the interaction of the  
883 template molecule with the cavity. Several methods of forming molecularly imprinted  
884 films, such as in situ polymerization, electrochemical polymerization, sol-gel, and  
885 self-assembly, have been employed to construct molecularly imprinted  
886 electrochemical sensors.

887 MIP-based potentiometric sensors, which rely on generating a potential  
888 difference across a membrane placed between two charged solutions with different  
889 activity without the extraction of template from the membrane, have been reported to  
890 have unique advantages that they do not require the template molecules to diffuse  
891 through the electrode membranes for generation of membrane potentials, thus  
892 obviously reducing the response time.<sup>115</sup> Based on this strategy, Liang *et al.* have  
893 explored a potentiometric sensor employing a new polymeric membrane ion-selective  
894 electrode based on a MIP for the selective analysis of melamine in milk.<sup>116</sup> In this  
895 work, the MIP was prepared through the non-covalent imprinting process by using  
896 melamine as a template molecule, methacrylic acid (MAA) as a functional monomer,  
897 ethylene glycol dimethacrylate (EGDMA) as a cross-linking agent, and

898 2,2'-azobisisobutyronitrile (AIBN) as an initiator. Melamine could bind with MAA  
899 through the triple hydrogen bonds. Removal of the template and unreacted monomers  
900 was done by washing the polymer successively in methanol/acetic acid solution.  
901 Melamine is readily protonated in aqueous solution at pH lower than 5.0, which could  
902 lead to the near-Nernstian response (54 mV/decade) of membrane electrode, realizing  
903 the determination of the melamine with the detection limit of 6  $\mu\text{M}$ .

904 The major drawback for MIP-based sensors is the difficulty in regenerating the  
905 MIP films. MIP films obtained by in situ polymerization are easily destroyed because  
906 of the collapse of special recognition cavities during the extraction template process,  
907 which in turn affects the sensor reproduction ability. In addition, the extraction  
908 process of template molecules is tedious and time-consuming. Pizzariello *et al.*  
909 proved that a renewable MIP sensor can be constructed by embedding MIP particles  
910 in a carbon paste.<sup>117</sup> Inspired by this strategy, a novel strategy for constructing highly  
911 sensitive and easily renewable MIP sensors for melamine detection was proposed.<sup>118</sup>  
912 MIP particles with melamine recognition cavities were designed and prepared based  
913 on the non-covalent method, and the imprinting process and removal of template were  
914 similar to the procedure mentioned in Ref.<sup>118</sup>. Film renewability was achieved by  
915 embedding MIP particles in a carbon paste using solid paraffin as an adhesive, and the  
916 high sensitivity was obtained using a highly sensitive enzyme amplifier. Melamine  
917 was indirectly determined from the competition between the reactions of melamine  
918 and horseradish peroxidase-labeled melamine with the vacant cavities. Thus the  
919 detection signals were amplified because of enzymatic reaction to the  $\text{H}_2\text{O}_2$  catalytic  
920 oxidation. Based on voltammetric monitoring and amplification of detection signals,  
921 sensitivity for the melamine determination was markedly improved with the detection  
922 limit of 0.7 nM. After each use, the sensor was easily renewed by simple mechanical  
923 polishing.

924 With  $[\text{Fe}(\text{CN})_6]^{3-/4-}$  as an electroactive probe, the MIPs sensor was successfully  
925 applied to the selective determination of melamine in milk products. For example,  
926  $[\text{Fe}(\text{CN})_6]^{3-/4-}$  was used for the indirect determination of melamine by Jin *et al.* on a  
927 molecularly imprinted nano-porous film based electrochemical sensor.<sup>119</sup> The



928 molecularly imprinted nano-porous sensing film was prepared by casting  
929 melamine-MIP on a nano-Ag polyquercetin modified electrode for the adsorption of  
930 melamine. The film displays excellent and highly selective sorption of melamine in  
931 the 3-dimensional porous nanomaterial. The electrode responds linearly to melamine  
932 in the concentration range of  $1 \times 10^{-8}$  to  $9 \times 10^{-7}$  M, with a detection limit of  $1.3 \times 10^{-9}$   
933 M (at  $3\sigma$ ) in real samples. The interaction between the porous film and melamine was  
934 also studied by using  $[\text{Fe}(\text{CN})_6]^{3-/4-}$  as an electrochemical indicator.

935 In addition to the traditional MIPs synthesized by in situ polymerization,  
936 molecular imprinting has been approached using the electrosynthesis of conducting  
937 polymers through galvanostatic, potentiostatic and cyclic voltammetric methods.<sup>120</sup>  
938 Electrosynthesis of MIP-based sensors allows the generation of a rigid, uniform and  
939 compact molecularly imprinted layer with good adherence to a transducer surface of  
940 any shape and size. Moreover, the thickness and the density of the polymer layer can  
941 also be well controlled with the electropolymerization conditions (*e.g.*, applied  
942 potential, the number of CV cycles). This feature gives the possibility of creating a  
943 direct communication between the coating and the surface of the transducer in a very  
944 simple way for the development of electrochemical sensors.<sup>121, 122</sup> Recently, MIPs  
945 prepared by electropolymerization have been applied in the electrochemical sensors  
946 for melamine monitoring as reported in the following assays.

947 A novel and simple electrochemical sensor has been developed for the  
948 determination of melamine in milk, which is based on the electropolymerized MIP of  
949 poly(para-aminobenzoic acid) (P-pABA) modified glassy carbon electrode using  
950  $[\text{Fe}(\text{CN})_6]^{3-/4-}$  as the electrochemical indicator.<sup>123</sup> p-ABA was chosen as the monomer  
951 for electropolymerization because it has been shown that it can be easily  
952 electropolymerized on various substrate materials and form films with good chemical  
953 and mechanical stability.<sup>124-127</sup> Meanwhile, pABA can establish hydrogen bonds with  
954 melamine, which facilitates the recognition and selectivity for the analyte. The  
955 (P-pABA) film was deposited in a pABA solution by potentiodynamic cycling of  
956 potential with the template (melamine) on a glassy carbon electrode. The surface  
957 feature of the modified electrode was characterized by EIS and CV. DPV was

958 employed for the quantitative determination of melamine with the detection limit of  
959 0.36  $\mu\text{M}$  due to its higher sensitivity compared with CV. The results of this research  
960 demonstrate that it is feasible to use the molecular imprinting methodology when  
961 preparing sensing devices for analytes that are electrochemically inactive.

962 A novel molecularly imprinted impedimetric sensor was promoted for selective  
963 detection of melamine with a low detection limit down to  $3.0 \times 10^{-9}$  M.<sup>128</sup> The Au  
964 electrode modified with MIP of poly (2-mercaptobenzimidazole) (PMBI) was  
965 prepared by electrochemical polymerization of 2-mercaptobenzimidazole (2-MBI)  
966 using CV in the presence of template molecule melamine. 2-Mercaptobenzimidazole  
967 (2-MBI) contained a mercapto group and might consequently improve the  
968 polymer-gold binding characteristics. The obtained poly(2-mercaptobenzimidazole)  
969 (PMBI) is very stable even under harsh conditions. The properties of the sensor were  
970 investigated by impedance spectroscopy, cyclic voltammetry and differential pulse  
971 voltammetry using  $[\text{Fe}(\text{CN})_6]^{3-/4-}$  as the electrochemical probe. The tailor-made  
972 cavities formed in the imprinted film showed good selectivity toward melamine, and  
973 the main driving force of recognition is the *p*-donor-acceptor interaction between  
974 melamine and PMBI. The effective method has a potential application to monitor  
975 nonelectrochemically active substances in complicated real samples.

976 Compared to the reported indirect electrochemical methods, direct detection of  
977 melamine should be much more simple and convenient. The imprinted sol-gel  
978 electrochemical sensor for direct recognition and detection of melamine in real  
979 samples has been explored without the need of indirect signal reporter such as  
980  $[\text{Fe}(\text{CN})_6]^{3-/4-}$ .<sup>129</sup> Thin film of molecularly imprinted sol-gel polymers with specific  
981 binding sites for melamine was fabricated on glassy carbon electrode surface by  
982 electropolymerization method. Electrochemical behavior of melamine on GCE  
983 surface was investigated in an acidic electrolyte, demonstrating that a pair of  
984 reversible redox peaks (0.65 V for reduction current and 0.72 V for oxidized current)  
985 could be seen, which was assumed to be the formation of a radical cation through  
986 electrochemical oxidation.<sup>130</sup> Then melamine could be detected by its reversible redox  
987 peaks instead of other electroactive probe. A change of oxidation peak of melamine

988 could be seen corresponding to the incorporation of melamine onto the surface of  
989 MIPs/GCE. Based on this strategy, melamine could be detected in the wider range of  
990  $6.3 \times 10^{-7}$  M to  $1.1 \times 10^{-4}$  M with a detection limit of  $6.8 \times 10^{-8}$  M.

### 991 **2.2.5 Others**

992 Based on the oxidation peak for melamine adsorption at 1.1 V, the oxidized  
993 polycrystalline gold electrode (poly GE) has been directly utilized for the detection of  
994 melamine in milk powder and human urine by DPV and impedimetry.<sup>131</sup> Using  
995 differential pulse polarography, a novel, sensitive and reliable method has been  
996 developed for melamine determination in milk and milk powder.<sup>132</sup> The peak of  
997 melamine at about -50 mV in pH 11.2 Britton-Robinson buffer electrolyte was used  
998 and the limit of detection and limit of quantification were obtained as 0.3 and 1.0  $\mu$ M,  
999 respectively.

1000 Recently, based on the synergetic effect of the electrochemical accumulation  
1001 process and the signal amplification of enzymes, a new sensitive method has been  
1002 developed for the detection of subnanomolar melamine in infant milk powders and  
1003 fish feed samples.<sup>133</sup> There are two steps involved in the sensor construction process:  
1004 (1) accumulation of melamine on an electrode by cyclic voltammetric method and (2)  
1005 chemical coupling of horseradish peroxidase (HRP) with the accumulated melamine  
1006 through the linkage of glutaraldehyde. The coupled HRP catalyzes the oxidation of  
1007 guaiacol to generate an amber-colored product. Quantitative analysis of melamine is  
1008 performed by measuring the absorption intensities of the colored product.

### 1009 **3. Biosensors for the analysis of melamine**

1010 A biosensor is an analytical device, used for the detection of an analyte, which  
1011 combines a biological component with a physicochemical detector. A biosensor  
1012 typically consists of a bio-recognition component, a biotransducer component, and an  
1013 electronic system which includes a signal amplifier, processor, and display. According  
1014 to the specific bio-recognition principle, biosensors are classified into  
1015 immunochemical, enzymatic, non-enzymatic receptor, tissues, organelles, microbes or  
1016 whole-cell and DNA biosensors, usually transformed by electrical, thermal or optical  
1017 signals.<sup>134</sup> Compared with conventional analytical techniques, biosensors offer the

1018 main advantages such as possibility of portability, miniaturisation and working on-site,  
1019 and the ability to measure pollutants in complex matrices with minimal sample  
1020 preparation.<sup>135</sup> Various biosensing methods developed for detection of melamine have  
1021 been discussed in the following sections.

### 1022 **3.1 Aptamer-based sensors**

1023 Aptamer is a synthetic single-stranded nucleic-acid or peptide molecules binding  
1024 to particular target with high affinity and specificity, which is normally screened with  
1025 a combinatorial technique called systematic evolution of ligands by exponential  
1026 enrichment (SELEX).<sup>136, 137</sup> Aptamers offer advantages over antibodies as they are  
1027 readily synthesized, possess desirable storage properties and could be modified easily.  
1028 Because of their inherent superiorities, they are widely used as recognition elements  
1029 in biosensor construction and are quite helpful in the detection of a wide range of  
1030 substances from metal ions, organic molecules, peptides, protein to cells.<sup>138, 139</sup>

1031 The ability of pyrimidine to form hydrogen bonds with purines has been well  
1032 documented, and the hydrogen bonding between thymine and  
1033 2,6-diamino-5-methylpyrimidin-4-one, which has a similar molecular structure as  
1034 melamine, was reported.<sup>140</sup> Thus, the single stranded oligonucleotide containing  
1035 thymines may also bind to melamine *via* hydrogen bonding. Based on this, numbers  
1036 of aptamer-based biosensors for melamine detection have been developed. Generally,  
1037 the selected aptamers are the single stranded oligonucleotide of thymines with the  
1038 difference on the length of the sequence.

1039 Huang *et al.* has firstly reported visual and light scattering spectrometric  
1040 detections of melamine with polythymine-stabilized AuNPs.<sup>141</sup> Citrate-coated AuNPs  
1041 get aggregated obviously in high ionic strength medium. While, polythymine can be  
1042 adsorbed onto the surfaces of AuNPs and make nanoparticles well-dispersed and  
1043 stable owing to the repulsion force of the neighboring nanoparticles resulting from the  
1044 negative charges of polythymine. If melamine, which might form triple H-bonds with  
1045 polythymine in aqueous medium and decrease the negative charges of the surface of  
1046 AuNPs, is added, then aggregation of AuNPs might occur, resulting in visual changes  
1047 from red to blue owing to the variation of localized plasmon resonance absorption and

1048 light scattering. Notably, it has been proved that single-stranded DNA oligomers  
1049 including polyA<sub>n</sub>, polyC<sub>n</sub>, polyG<sub>n</sub> and polyT<sub>n</sub> could make AuNPs stable without  
1050 aggregation owing to enough negative charges on their surface. However, the  
1051 presence of melamine in the medium only makes the polyT<sub>n</sub>-stabilized AuNPs  
1052 aggregate, indicating that specific interactions occur between melamine and polyT<sub>n</sub>.  
1053 And the stability of a single base unit in polyT<sub>n</sub> decreases with the length increase of  
1054 the polyT<sub>n</sub>. It was the first report which demonstrated the novel specific recognition of  
1055 melamine with thymine and this triple H-bonds motif in aqueous medium.

1056 Later, He *et al.* has developed an aptamer-AuNPs-based colorimetric sensor  
1057 using label-free and labeled AuNPs.<sup>142</sup> In the labeled-free AuNPs procedure (as shown  
1058 in Fig. 5), AuNPs were coated by the negative-charged citrate ions which could  
1059 prevent AuNPs from aggregation in aqueous solution, while induce the AuNPs  
1060 aggregation in the presence of high concentration of salt. However, aptamers  
1061 (poly-T<sub>10</sub>) could strongly adsorb on AuNPs and enhance the stability of AuNPs  
1062 against the NaCl-induced aggregation. In the presence of melamine, aptamers will  
1063 competitively bind with melamine by the stronger affinity which will decrease the salt  
1064 tolerance of AuNPs and will result in the subsequent aggregation of AuNPs. The color  
1065 of AuNPs solution quickly changed from wine red to blue as a result of aggregation  
1066 that provides a rapid and on-site detection of melamine by naked eyes or UV-Vis  
1067 spectrometer. However, in the labeled-based AuNPs procedure, the single-stranded  
1068 oligonucleotide labeled AuNPs was used for melamine determination, which was also  
1069 based on the combination of thymine with melamine. The HSsDNA  
1070 (HS-(CH<sub>2</sub>)<sub>6</sub>-TAGCTATGGAATTCCTCGTAGGCATTTTTT) was first attached to the  
1071 surface of AuNPs. The DNA functionalized AuNPs can assemble when the  
1072 oligonucleotides hybridize, which causes the changes of colors. Melamine could  
1073 induce the hybridization. When melamine was added in, the functionalized AuNPs  
1074 assembled upon binding of the oligonucleotide to melamine, which resulted in the  
1075 red-to-blue color change. Particularly, this assembly process was reversible. The  
1076 dissociation would occur upon thermal denaturation, leading to a blue-to-red color  
1077 change. Both assays were high selectivity and high sensitivity with the detection limit

1078 as low as 41.7 nM and 46.5 nM, respectively. Notably, compared with label-free  
1079 method, the label-based method provides a better stability, a better accuracy and a  
1080 larger response range.

1081 Similarly, an AuNPs-based colorimetric aptasensor for melamine was developed  
1082 using salt-induced aggregation of AuNPs.<sup>143</sup> In this paper, they used  
1083 5'-TTTTTTTTTTTTTTTTTTTT-3'(dT20) as melamine aptamer. It was used to  
1084 protect AuNPs under conditions of high salt concentrations. After adding melamine,  
1085 melamine would competitively combine with the aptamer and induced the release of  
1086 aptamer from the surface of AuNPs. Without the protection of aptamer, the  
1087 aggregation of AuNPs will cause the color change. The detection limit was 1.5 mg/L  
1088 in naked eyes and 0.5 mg/L with UV-Vis spectrometer.

1089 Recently, Zhou *et al.* reported an AuNPs-based colorimetric aptasensor for  
1090 melamine which is different from others.<sup>144</sup> They indicated that some approaches  
1091 using modified nanoparticles and high concentrations of NaCl as the sensor had a  
1092 shortcoming that the interference of other salts cannot be ignored. This study  
1093 exhibited the great advantages of cationic polymers in the aggregation of AuNPs. Poly  
1094 (diallyldimethylammonium chloride) (PDDA), a water soluble cationic polymer,  
1095 exhibited two features in the present biosensor. First, it can be used to aggregate  
1096 citrate-stabilized AuNPs. As a positively charged polyelectrolyte, PDDA can be used  
1097 to aggregate the AuNPs or stabilize the AuNPs-ssDNA, depending on whether or not  
1098 melamine is present. Second, it can interact with an aptamer to form a complex  
1099 structure. In the absence of melamine, the aptamer can combine with both the AuNPs  
1100 by intermolecular and hydrophobic forces and PDDA to form a complex structure, so  
1101 that the AuNPs do not aggregate and change the solution color. In the presence of  
1102 melamine, the T base and melamine could form many hydrogen bonds, thus, the  
1103 ssDNA and melamine could form stable conjugates. As a result the aptamer lost the  
1104 ability to protect the AuNPs from PDDA resulting in the aggregation of AuNPs.  
1105 Hence, they used PDDA to control the aggregation of the AuNPs instead of NaCl  
1106 which makes the system more stable, selective and sensitive.

1107 The resonance scattering (RS) analysis is a new, rapid, simple, convenient and

1108 sensitive analytical technique and was applied to the analysis of trace nucleic acid,  
1109 protein, drug and so on.<sup>145</sup> The RS effect of nanoparticles was combined with a highly  
1110 selective aptamer reaction to assay  $\text{Hg}^{2+}$  and  $\text{K}^+$  with satisfactory results.<sup>146-148</sup> A RS  
1111 spectral assay was developed using aptamer-modified AgNPs as probe.<sup>149</sup> AgNPs was  
1112 modified by a single-strand DNA to fabricate an Ag-aptamer probe for melamine. In  
1113 the presence of NaCl, the probe was stable. While, upon the addition of melamine, it  
1114 interacted with the probe to aggregate big clusters, which caused a significant increase  
1115 of the RS intensity at 470 nm. The increased RS intensity is linear to melamine  
1116 concentration in the range of 6.31-378.4  $\mu\text{g/L}$  with a detection limit of 3.1  $\mu\text{g/L}$ .

1117 Later, a similar but more sensitive strategy has been established by the same  
1118 group with the AuNPs instead of AgNPs.<sup>150</sup> The aptamer was used to label AuNPs to  
1119 fabricate an aptamer-AuNPs probe for melamine. The probe was stable in buffer  
1120 solutions and in the presence of high concentration of electrolyte. Upon addition of  
1121 melamine, it interacted with the probe to form big aptamer-AuNPs-melamine  
1122 aggregations that led to the RS intensity at 566 nm increased greatly. The increased  
1123 RS intensity is linear to melamine concentration in the range of 1.89-81.98  $\mu\text{g/L}$ , with  
1124 a detection limit of 0.98  $\mu\text{g/L}$  melamine. In addition, in this paper, the method has  
1125 been improved based on the high affinity between aptamer and AuNPs. The unreacted  
1126 probe in the aptamer reaction solution exhibited strong catalytic effect on the slow  
1127  $\text{Cu}_2\text{O}$  particle reaction between glucose and Fehling reagent, but the catalytic activity  
1128 of AuNPs aggregations is very weak. In addition, the cubic  $\text{Cu}_2\text{O}$  particles produced  
1129 and exhibited a RS peak at 614 nm. When melamine concentration increased, the  
1130 unreacted aptamer-AuNPs probe decreased, and the RRS intensity decreased. The  
1131 decreased RS intensity is linear to melamine concentration in the range of 0.63-47.30  
1132  $\text{ng/L}$  melamine, with a detection limit of 0.38  $\text{ng/L}$ . The proposed aptamer-modified  
1133 AuNPs catalytic RS assay was more sensitive and selective for melamine  
1134 determination.

### 1135 **3.2 Immunosensors**

1136 Immunoassay is a kind of analytical technique which mainly depends on the  
1137 immunoaffinity of an antibody towards its antigen, and the extent of binding can be

1138 converted to readable output signals using an appropriate transducer.  
1139 Immunoassay-based biosensors are usually fabricated using monoclonal, polyclonal  
1140 or recombinant antibodies as biorecognition elements.<sup>151</sup> These immunosensors have  
1141 been widely applied in pharmaceutical analysis, toxicological analysis, bioanalysis,  
1142 clinical chemistry, and environmental analysis, due to their advantages such as high  
1143 sensitivity, high selectivity, rapid detection and possible analysis of difficult matrices  
1144 without extensive pretreatment.

### 1145 **3.2.1 Enzyme-linked immunosorbent assay (ELISA)**

1146 Enzyme-linked immunosorbent assay (ELISA) uses the basic immunology  
1147 concept of an antigen binding to its specific antibody. Subsequently the antigen is  
1148 detected by a secondary, enzyme-coupled antibody. A chromogenic substrate for the  
1149 enzyme yields a visible color change or fluorescence, indicating the presence of  
1150 antigen. The key step of ELISA is the direct or indirect detection of antigen by  
1151 adhering or immobilizing the antigen-specific capture antibody directly onto the well  
1152 surface.<sup>152</sup> In comparison to other biological quantification techniques, the major  
1153 advantage of ELISA is that it can realize the detection of antigens at low  
1154 concentrations, and it has been widely used for the detection of very small quantities  
1155 of biological molecules such as proteins, peptides, hormones, or antibody in the food  
1156 and environmental analyses.<sup>153-156</sup> Generally, ELISA is classified into three common  
1157 types: indirect ELISA, sandwich ELISA and competitive ELISA. Many ELISAs have  
1158 been reported for the determination of melamine. Among them, indirect competitive  
1159 enzyme-linked immunosorbent assay (icELISA) has been widely developed due to its  
1160 high sensitivity to compositional differences in complex antigen mixtures, even when  
1161 the specific detecting antibody is present in relatively small amounts. Horseradish  
1162 peroxidase (HRP) and tetramethylbenzidine (TMB) are usually used as the labeling  
1163 enzyme and the substrate, respectively. Melamine, as a kind of hapten, has no  
1164 immunogenicity and should be conjugated to a protein to add immunogenicity.  
1165 Therefore, it is one of the key steps to produce a complete antigen for the  
1166 development of immunoassays. Bvine serum albumin (BSA) and ovalbumin (OVA)  
1167 are commonly used to be conjugated to melamine.



1168 Wang *et al.* proposed an icELISA for the simultaneous determination of  
1169 melamine and cyromazine.<sup>157</sup> Cyromazine is a triazine pesticide used for fly control in  
1170 crop production and animal feed to inhibit insect growth, whereas melamine is the  
1171 major metabolite of cyromazine. Thus, cyromazine and melamine can exist  
1172 simultaneously in animal-derived food. In this paper, they obtained the polyclonal  
1173 antibody showing broad specificities to melamine and cyromazine by immunising  
1174 three rabbits with the melamine-BSA conjugate. Another melamine conjugate,  
1175 malmine-OVA was also produced to be the coating antigen for the icELISA. HRP  
1176 labeled goat anti-rabbit IgG and TMB were added as the secondary antibody and the  
1177 substrate, respectively. This is the first paper reporting the development of an  
1178 icELISA method for the simultaneous detection of melamine and cyromazine in  
1179 animal muscle tissues. The limit of detection for melamine and cyromazine was 1.8  
1180 ng/g and 4.5 ng/g, respectively, and the cross-reactivity (CR) was 59%.

1181 Immunoassay with high CR is suitable for multi-residue analysis, however, it is  
1182 not expected in a single-analyte specific analysis. Due to the similar structure to  
1183 melamine, cyromazine is a major potential matrix factor which is not expected in the  
1184 immunochemical analysis of melamine. Sun *et al.* developed ciELISAs for melamine  
1185 detection by synthesizing several melamine haptens with different spacer-arms and  
1186 coupling them to BSA and OVA for immunogens and coating antigens,  
1187 respectively.<sup>158, 159</sup> Polyclonal antibodies were obtained for evaluating homogeneous  
1188 and heterogeneous assay formats. In both studies, the specificity and sensitivity of  
1189 icELISAs was greatly improved using the heterologous combination of coating  
1190 antigen and antibody, while the CR for cyromazine was significantly decreased.  
1191 Notably, it is interesting to find that spacer arm effects and electronic effects appear to  
1192 be two important factors with regard to the antibody binding to the haptens.

1193 A monoclonal antibody (mAb)-based icELISA has been developed for the  
1194 analysis of melamine.<sup>160</sup> Melamine was conjugated with BSA and OVA for  
1195 immunogen and coating antigen, respectively. Melamine-BSA immunogen was used  
1196 to immunise the mice and then the mAb against melamine was obtained. Goat  
1197 anti-mice IgG peroxidase conjugate and TMB were added as the secondary antibody

1198 and the substrate, respectively. The cross-reactivity with cyromazine or other  
1199 compounds was not studied in this paper. While the proposed method presents high  
1200 sensitivity with a detection limit of 0.01 ng/mL, and it has been successfully applied  
1201 in the liquid milk, powder milk, dog food and cat food indicating that it is a potential  
1202 method for the rapid and reliable monitoring of melamine in real samples.

1203 Another mAb based icELISA for the determination of melamine has been  
1204 established based on rational hapten modification and heterogeneous antibody/coating  
1205 antigen combinations.<sup>161</sup> Three melamine derivatives with different length of  
1206 carboxylic spacer at the end were synthesized and linked to carrier proteins for the  
1207 production of immunogens (melamine-BSA) and coating antigens (melamine-OVA).  
1208 Mice were immunized with immunogen and mAb against melamine was produced.  
1209 The results showed that, in heterogeneous format, the antibody will have a higher  
1210 affinity toward the analyte in comparison to the coating antigen, leading to a higher  
1211 sensitivity. Thus a highly sensitive and specific ELISA using heterogenous  
1212 antibody/coating antigen combinations was established. The CRs of the assays with  
1213 cyromazine were within 8.2 % and no cross-reactivity with other structurally related  
1214 and unrelated compounds was found.

1215 A novel immunoassay using 2 types of sensors (QDs and an enzyme) was  
1216 simultaneously used for detecting multiple structurally different molecules in milk,  
1217 including melamine, sulfonamides and quinolones.<sup>162</sup> The method integrates the  
1218 indirect competitive fluorescence-linked immunosorbent assay (icFLISA) using  
1219 QD605 and QD655 as probes and an icELISA using HRP labeled secondary antibody.  
1220 Compared to icELISA, icFLISA is the assay which utilizes fluorescent material as the  
1221 only sensitive fluorescent label of the sensor system instead of enzyme. In this study,  
1222 the icFLISA was produced by anti-sulfonamide and anti-quinolone broad-specificity  
1223 mAbs for simultaneously detecting 6 sulfonamides and 11 quinolones. Combined with  
1224 the icFLISA, an icELISA was utilized for detecting melamine from the same milk  
1225 samples. The cross-reactivity of the mAbs was retained while binding the QDs by  
1226 using avidin and a secondary antibody as bridges. Milk samples were detected using  
1227 this hybrid immunoassay, with limits of detection of the quinolones (0.18 ng/mL),

1228 sulfonamides (0.17 ng/mL) and melamine (7.5 ng/mL), respectively. The results  
1229 demonstrated that the detection limits of the integrated methods were better than  
1230 required and simplified the sample pretreatment process. The developed novel  
1231 immunoassay based on icFLISA in conjunction with the traditional icELISA is  
1232 suitable for high-throughput screening of low-molecular weight contaminants.

1233 Later, Sanz-Medel *et al.* established a competitive FLISA for melamine analysis  
1234 based on the synthesis and characterization of a new immunoprobe,  
1235 melamine-BSA-QDs conjugates.<sup>163</sup> Melamine was firstly conjugated with BSA for the  
1236 production of melamine-BSA conjugates. The carbodiimide chemistry was further  
1237 used to synthesize the immunoprobe melamine-BSA-QD forming a chemical bond  
1238 between the carboxylic groups from the polymeric coating of the QDs and the amino  
1239 groups from the BSA. Thus, QDs were conjugated to the antigen and a competitive  
1240 immunoassay format was selected for determination of melamine, where the hapten  
1241 and the immunoprobe (melamine-BSA-QDs) compete for the limited binding sites of  
1242 the immobilized antibody. The competition is established by the addition of a mixture  
1243 of the standard (or sample) and a known amount of the immunoprobe  
1244 (melamine-BSA-QD). The fluorescence emission of the photoactivated QDs from the  
1245 melamine-BSA-QDs recognised by the antibody is measured as the analytical signal  
1246 of this competitive immunoassay. This method combined the advantages of an ELISA  
1247 immunoassay (simple sample preparation and high throughput) with the unique  
1248 properties of fluorescent QDs to develop a convenient quantitative analysis of  
1249 melamine in infant formula milk.

### 1250 **3.2.2 Immunochromatographic assay**

1251 The concept of immunochromatography is a combination of chromatography  
1252 (separation of components of a sample based on differences in their movement  
1253 through a sorbent) and immunochemical reactions. Immunochromatography combines  
1254 the speed of a homogeneous immunoassay with the separation of reacted and  
1255 unreacted compounds by a variety of heterogeneous methods. Another advantage of  
1256 immunochromatography is that the fluid flow through the carrier (*e.g.*, sorbent and  
1257 membrane) enables separation of reacted from unreacted products without the need

1258 for additional precipitation or washing steps. Immunochromatographic analyses are  
1259 rapid and simple, allowing for point-of-care testing. The most widespread  
1260 immunochromatographic system is the test strip which is an assembly of several plain  
1261 porous carriers impregnated with immunoreagents. On contact with the test strip, a  
1262 liquid sample flows along the carriers, and detectable immune complexes are formed  
1263 in certain zones of the test strip. Immunochromatographic test strips are mass  
1264 produced, and are widely used for the detection of pregnancy, for drug screening, to  
1265 identify markers for various diseases, and for a number of other analytical tasks.<sup>164</sup>

1266 An immunogold chromatographic strip tests have been developed for detecting  
1267 melamine.<sup>165</sup> The capture reagents, melamine-BSA antigen and goat anti-mouse IgG,  
1268 were immobilized on the nitrocellulose (NC) membrane in the test line and control  
1269 line, respectively. MAb was labeled with colloidal gold and used as detection reagents.  
1270 The principle of test strips is based on competitive binding immunoassay. If melamine  
1271 was absent in the sample, the detection reagent would then be trapped by the capture  
1272 reagent to form a visible test line. If melamine was present in the sample, then it  
1273 would compete with the capture reagent for the limited amount of detection reagent.  
1274 When enough melamine was present, it would then prevent the detection reagent from  
1275 binding the capture reagent, and the test line signal would decrease to a nonvisible  
1276 line and the results would be positive. When the test procedure was properly  
1277 performed, the control line was always visible. The limit of detection was estimated to  
1278 be 0.05  $\mu\text{g/mL}$  in raw milk, since the detection test line on the strip test completely  
1279 disappeared at this concentration. The limit of detection was 2  $\mu\text{g/mL}$  (or 2  $\mu\text{g/g}$ ) for  
1280 milk drinks, yogurt, condensed milk, cheese, and animal feed and 1  $\mu\text{g/g}$  for milk  
1281 powder. Compared with the ELISA, the immunogold chromatographic assay requires  
1282 the least sample pretreatment, without the need for expensive equipment, and the  
1283 results can be obtained within 3-5 min. It is the first report concerned with the method  
1284 of immunogold chromatographic assay for detection of melamine in raw milk, milk  
1285 products and animal feed.

1286 A rapid and sensitive lateral flow immunoassay (LFIA) based on competitive  
1287 format was developed and validated for simultaneous detection of cyromazine and

1288 melamine in foods of animal origin.<sup>166</sup> The principle of test strips is based on  
1289 competitive binding immunochromatographic assay, in which the reporter reagents in  
1290 the conjugate pad were anti-cyromazine mAbs and anti-melamine mAbs coated with  
1291 colloidal gold particles. The cyromazine-BSA, melamine-BSA and goat anti-mouse  
1292 IgG were separately immobilised on nitrocellulose membranes as the capture reagents.  
1293 This paper first reported an immunogold chromatographic method for the  
1294 simultaneous determination of melamine and cyromazine in foods of animal origin.  
1295 The sample preparation was simple and the sensitivity was high with the lower  
1296 detection limit of 1.75 and 2.04 ng/g for cyromazine and melamine, respectively.  
1297 Therefore, the lateral flow immunoassay can be used as a simple, semiquantitative,  
1298 quantitative and sensitive screening tool for routine monitoring the residues of  
1299 cyromazine and/or melamine in large number of animal food products.

1300 In contrast with a colloidal gold test strip for melamine, the lateral flow test strip  
1301 based on colloidal selenium immunoassay for rapid detection of melamine was easy  
1302 to prepare and more cost-efficient.<sup>167</sup> Colloidal selenium was synthesized by  
1303 L-ascorbic acid to reduce seleninic acid at room temperature. The mAb was  
1304 conjugated with colloidal selenium instead of colloidal gold because of the relatively  
1305 complicated preparation process and high cost of gold particles. The test  
1306 line-immobilized melamine-BSA can react with mAb, thus capturing adequate  
1307 colloidal selenium particles to show an orange test line. If there is elevated melamine  
1308 in the tested sample, the melamine will react with mAb first, leaving insufficient mAb  
1309 for melamine-BSA to bind, hence no visible test line can be observed due to lack of  
1310 colloidal selenium particles. The intensity of the test line color is proportionate to the  
1311 quantity of melamine in the sample. Similarly, the immobilized goat anti-mouse IgG  
1312 in the control area will always react with mAb to show an orange line. The positive  
1313 result is determined by the appearance of an orange line in the control area, but the  
1314 absence of it in the test area. The negative result is determined by an orange line  
1315 exhibited in both the test area and the control area. If no visible orange line is present  
1316 in the control area, the test strip is considered invalid regardless of whether an orange  
1317 line appears in the test area or not. The detection limit of the test strip reached 150

1318  $\mu\text{g}/\text{kg}$ , 1,000  $\mu\text{g}/\text{kg}$ , and 800  $\mu\text{g}/\text{kg}$  in liquid milk, milk powder, and animal feed,  
1319 respectively. No cross-reactions with homologues cyanuric acid, cyanurodiamide, or  
1320 ammeline were found. Moreover, the melamine test strip can remain stable after  
1321 storage for 1 year at room temperature. This study firstly employed a colloidal  
1322 selenium-based chromatographic immunoassay for detection of melamine in milk,  
1323 milk powder, and animal feed.

### 1324 **3.2.3 Optical immunosensors**

1325 Optical immunosensor generally comprises transducer, which can convert the  
1326 signals from antibody and antigen binding to light signals, and it is classified into  
1327 surface-plasmon resonance (SPR) and fluorescence biosensors. SPR is an  
1328 electromagnetic phenomenon resulting from the interaction of incident light with free  
1329 electrons at a metal-dielectric interface. SPR sensors directly measure the changes in  
1330 refractive index occurring at the surface of a metal film. SPR biosensors have become  
1331 an established technology for observation of biomolecular interactions.  
1332 Biorecognition elements, such as antibodies and receptors, are immobilized on the  
1333 metal film supporting a surface Plasmon and are used to increase the specificity of  
1334 sensors. Adsorption of target species on the metal surface causes an increase in  
1335 refractive index, which induces a shift in the wavelength of the refracted wave.  
1336 Changes in the wave properties are measured using thin-film refractometers. Up to  
1337 now, SPR biosensors have been successfully applied for the detection of analytes  
1338 related to medical diagnostics, environmental monitoring, and food safety and  
1339 security.<sup>168, 169</sup>

1340 Fodey *et al.* have generated a polyclonal antibody based SPR biosensor for  
1341 detecting melamine.<sup>170</sup> As a result of its low molecular weight, melamine must be  
1342 coupled to a large carrier protein so that the conjugate will illicit an immune response  
1343 in the host animal. Preparation of such a conjugate is complicated by the small  
1344 chemical structure of melamine and the three amine groups that are available for  
1345 reaction with a protein. A structural mimic (6-hydrazino-1,3,5-triazine-2,4-diamine)  
1346 for melamine was used as a hapten for antibody production, removing the need for  
1347 chemical manipulation of melamine itself. A suitable bifunctional cross-linker was

1348 attached to the carrier protein to allow direct reaction with the hydrazide group of the  
1349 hapten. The resulting polyclonal antibody was then incorporated into a SPR optical  
1350 biosensor immunoassay. The antibody did not cross-react with any of the byproducts  
1351 of melamine manufacture; however, significant cross-reactivity was observed with the  
1352 insecticide cyromazine of which melamine is a metabolite. When sample matrix was  
1353 applied to the assay, a limit of detection of  $< 0.5 \mu\text{g/mL}$  was determined in both infant  
1354 formula and infant liquid milk.

1355 *Li et al.* have also developed a portable miniaturized SPR biosensor for rapid  
1356 detection and quantification of melamine through immunoassay based on the binding  
1357 between melamine and anti-melamine antibody.<sup>171</sup> With sensing surface comprising of  
1358 an avidin monolayer and biotinylated anti-melamine antibody, three types of  
1359 immunoassay have been successfully performed for the detection and quantification  
1360 of melamine, namely direct assay, displacement assay and competitive assay. In  
1361 addition to direct assay based on antibody-antigen binding, BSA-melamine conjugate  
1362 is used to induce more significant changes in displacement assay and competitive  
1363 assay. The displacement assay involves the introduction of an excess of the  
1364 BSA-melamine conjugate over the sensor surface to occupy as many binding sites as  
1365 possible. Upon addition of molecular melamine, displacement of the melamine-BSA  
1366 conjugate occurs. On the other hand, the competitive assay involves the introduction  
1367 of a mixture of the molecular melamine and melamine-BSA over the sensor surface  
1368 for them to compete for the binding sites. Compared to direct assay, the displacement  
1369 assay and competitive assay using BSA-melamine conjugate enhance the sensitivity  
1370 by about 14 times and 60 times, respectively. The competitive assay can be finished in  
1371 15 min with detection limit of  $0.02 \mu\text{g/mL}$ . The feasibility of testing real samples is  
1372 proven good for infant formula after simple pretreatment. The SPR biosensor with  
1373 proposed analysis assays is rapid, convenient and low-cost for effective detection of  
1374 melamine.

1375 In addition, several fluorescence immunosensors for detecting melamine have  
1376 been established. *Lei et al.* have designed a fluorescence polarization immunoassay  
1377 (FPIA) based on a polyclonal antibody for the determination of melamine in milk and

1378 milk powder.<sup>172</sup> FPIA is one of the most extensively used homogeneous techniques,  
1379 and meets the requirements of a simple, reliable, fast, and cost effective analysis.  
1380 FPIA is a competitive immunoassay method based on the increase in the polarization  
1381 of the fluorescence of a small fluorescein-labeled hapten (tracer) when it is bound by  
1382 a specific antibody. Recently, the use of FPIA for the determination of pesticides,  
1383 biological toxins, mycotoxins, and veterinary drugs in agricultural products and  
1384 environmental samples has been reported. The assay in this paper is based on an  
1385 improved polyclonal antibody produced by a melamine hapten  
1386 (6-hydrazinyl-1,3,5-triazine-2,4-diamine, hapten A) coupled to BSA as the  
1387 immunogen for the rabbit immunization. Three fluorescein-labeled melamine tracers  
1388 with different structures and spacer bridges were synthesized. Without any additional  
1389 coupling reagent, hapten A was linked directly to FITC (Fluorescein isothiocyanate  
1390 isomer I) for use as fluorescein-labeled tracer A. Tracers B and C were synthesized  
1391 using the active ester method based on hapten B (3-  
1392 (4,6-Diamino-1,6-dihydro-1,3,5-triazin-2-ylthio) propanoic acid) and hapten C (6-  
1393 (4,6-diamino-1,6-dihydro-1,3,5-triazin-2-ylamino) hexanoic acid) respectively. Thus,  
1394 tracers A, B, and C differed in not only the spacer length, but also in chemical  
1395 structure between the hapten and the fluorophore. All three tracers were used as the  
1396 competing molecules in the FPIA. The results showed that tracer C, with a six-carbon  
1397 spacer arm as a heterogeneous competitor, gave better assay sensitivity. This FPIA  
1398 method could realize the detection without complicated cleanup and it is the first  
1399 development of an FPIA for the detection of melamine.

1400 Another fluorescence immunosensor has been developed by Shi *et al.*<sup>173</sup> They  
1401 developed an indirect competitive immunoassay using the planar waveguide  
1402 fluorescence immunosensor (PWFI) based on the principle of immunoreaction and  
1403 total internal reflect fluorescence (TIRF). The objective of achieving spatially  
1404 resolved excitation and collection of fluorescence from fluorescently labeled  
1405 antibodies locally bound at a planar interface can be met by the evanescent field  
1406 excitation of fluorophore. Excitation light was guided by total internal reflection  
1407 within transducer structure resulting in an evanescent wave which allows the



1408 excitation fluorophore bound to the transducer surface. The TIRF principle allows  
1409 selective detection of surface bound fluorophore and, therefore, on line monitoring of  
1410 binding events, which was superior than that with direct illumination of the active  
1411 area of transducers. A planar transducer was also preferred to a fiber-based system, as  
1412 being manufactured as an integrated part to fluidics systems. For the detection of  
1413 melamine, an inhibition immunoassay was used. The Cy5.5 labeled  
1414 melamine-antibody was firstly mixed with analyzed samples for pre-incubation. The  
1415 antibody binding sites were occupied depending on the concentration of the melamine.  
1416 Then the mixture will pump through the sensor instrument and the free  
1417 melamine-antibody-Cy5.5 will bind the surface with immobilized melamine-BSA  
1418 conjugate. Since the melamine inhibited the antibodies binding to the immobilized  
1419 conjugate, the PWF I signal declined when concentrations of analyte increased. The  
1420 chip of the sensor immobilized by melamine-BSA was reusable and highly resistive to  
1421 non-specific binding of proteins.

#### 1422 **4. Perspective and conclusion**

1423 Several novel methods have been exhibited in above discussion including optical  
1424 sensors, electrochemical sensors and biosensors. These sensors possess the  
1425 advantages of sensitivity, rapidity, cheapness and are available for detection of  
1426 melamine in real samples such as raw milk, infant formula, meat, and animal feeds.  
1427 Nevertheless, they still require improvements in order to obtain robust and further  
1428 application.

1429 Metal nanoparticles-based colorimetric assays, which are simple and rapid, have  
1430 several drawbacks, including complicated pretreatment of real samples to remove the  
1431 interference components, instability of some functionalized metal nanoparticles, poor  
1432 selectivity and availability. Fluorescence sensors are still needed to be improved by  
1433 means of synthesising inorganic nanomaterials with homogeneous optical properties,  
1434 proposing novel modification strategies for nanomaterials to achieve better water  
1435 solubility and surface functionalization, enhancing the characterization methods, and  
1436 improving the purifying methods to increase the stability and chemical purity of  
1437 nanomaterials. Chemiluminescence sensors are promising methods for melamine

1438 detection due to the rapidness and controllable emission rate. However, many  
1439 chemiluminescence reactions exhibit low selectivity as a result of the interference  
1440 effects, and show low robustness for many experimental conditions such as pH,  
1441 temperature, reagent concentrations, nature of solvent, ionic strength, *etc.* Hence, the  
1442 practical applications of chemiluminescence sensors in real samples are in great  
1443 demand. Electrochemical sensors are endowed with low energy consumption, rapid  
1444 response time, enhanced selectivity, and refreshability. However, the poor  
1445 electroactivity of melamine limits the application of electrochemical sensors. Thus,  
1446 it's necessary to fabricate or utilize various electrochemical probes to realize the  
1447 determination of melamine indirectly. Immunosensors are based on the binding  
1448 properties of antibodies with antigens. The main drawbacks of this technique are that  
1449 a known reciprocal antigen or antibody must be generated to detect a given antibody  
1450 or antigen, and nonspecific binding of the antibody or antigen might lead a false result.  
1451 It is difficult to prepare antibodies with sufficiently high specificity to distinguish  
1452 compounds that are structurally closely related. For melamine screening, the  
1453 cross-reactivity to the insecticide cyromazine couldn't be ignored. Particularly,  
1454 melamine, as a kind of hapten, has no immunogenicity and should be conjugated to a  
1455 protein to add immunogenicity. Therefore, it is one of the key steps to produce a  
1456 complete antigen for the development of immunoassays for the melamine detection.

1457       It can be found that the establishment of various methods for melamine detection  
1458 is mainly based on the specific structure of melamine. For example, aptamer-based  
1459 sensors are developed on the basis of the formation of H-bonds between melamine  
1460 and T-base group of aptamer. Moreover, due to the similar structure, melamine could  
1461 replace the TPA in the  $\text{Ru}(\text{bpy})_3^{2+}/\text{TPA}$  ECL system and then realize the detection of  
1462 melamine by electrochemical sensing.

1463       It is evident that the novel materials, such as metal nanoparticles, aptamers,  
1464 quantum dots, graphene and carbon nano tube have good potential to be used for the  
1465 fabricating chemical and biosensors. Nonomaterials could realize the signal  
1466 amplification of sensors like optical sensors and electrochemical sensors, and then  
1467 improve the sensitivity of the method. Aptamers have the inherent characteristics of

1468 high recognition towards specific molecular targets, which could increase the  
1469 selectivity of the assay. Thus, aptasensors are increasingly replacing conventional  
1470 immuno-based sensing systems. Recently, relying on the specific identification of  
1471 aptamer and the advantages of nanomaterials including the unique optical and  
1472 electrochemical properties, our group has explored a variety of aptamer-based  
1473 nanosensors for the determination of noxious substances in food. Furthermore, our  
1474 group has made important progress and gradual achievement. Importantly, the  
1475 proposed methods would pave promising ways for the establishment of more novel  
1476 and effective strategies available for on-site screening, greatly expanding the practical  
1477 application of aptamer-based sensors.

1478 Compared to traditional method like chromatographic technique, novel sensors  
1479 may help the regulatory agencies and other people to monitor and to screen real  
1480 samples for the presence of melamine with less effort. Nevertheless, in spite that the  
1481 development of the sensors is rapidly and convincing, improvements in real sample  
1482 analysis still need to be focused on designing ideal sensing systems with better  
1483 sensitivity and selectivity towards melamine. Since the fabrication of sensors involve  
1484 various streams of science, multidisciplinary effort is necessary in designing ideal  
1485 sensors.

#### 1486 **Acknowledgements**

1487 This work was financially supported by the National Natural Science Foundation of  
1488 China (No. 20905031), the Natural Science Foundation of Jilin Province (No.  
1489 201215024) and the Excellent Youth Talent Cultivation Project of Heping Campus of  
1490 Jilin University.

1491

1492

1493

1494

1495

1496

1497

1498 **References**

- 1499 1 V. D. M. Finete, M. M. Gouvea, F. F. D. Marques and A. D. P. Netto, *Talanta*, 2014, **123**,  
1500 128-134.  
1501
- 1502 2 W. C. Andersen, S. B. Turnipseed, C. M. Karbiwnyk, S. B. Clark, M. R. Madson, C. M. Gieseke,  
1503 R. A. Miller, N. G. Rummel and R. Reimschuessel, *J. Agr. Food Chem.*, 2008, **56**, 4340-4347.  
1504
- 1505 3 E. Y. Y. Chan, S. M. Griffiths and C. W. Chan, *Lancet*, 2008, **372**, 1444-1445.  
1506
- 1507 4 N. Guan, Q. F. Fan, J. Ding, Y. M. Zhao, J. Q. Lu, Y. Ai, G. B. Xu, S. N. Zhu, C. Yao, L. N.  
1508 Jiang, J, Miao, H. Zhang, D. Zhao, X. Y. Liu and Y. Yao, *N. Engl. J. Med.*, 2009, **360**, 1067-1074.  
1509
- 1510 5 F. Sun, W. Ma, L. Xu, Y. Zhu, L. Liu, C. Peng, L. Wang, H. Kuang and C. Xu. *TrAC-Trends Anal.*  
1511 *Chem.*, 2010, **29**, 1239-1249.  
1512
- 1513 6 T. Kobayashi, A. Okada, Y. Fujii, K. Niimi, S. Hamamoto, T. Yasui, K. Tozawa and K. Kohri,  
1514 *Urol. Res.*, 2010, **38**, 117-125.  
1515
- 1516 7 A. K. Hau, T. H. Kwan and P. K. Li, *J. Am. Soc. Nephrol.*, 2009, **20**, 245-250.  
1517
- 1518 8 C. A. Brown, K. S. Jeong, R. H. Poppenga, B. Puschner, D. M. Miller, A. E. Ellis, K. Kang, S.  
1519 Sum, A. M. Cistola and S. A. Brown, *J. Vet. Diagn. Invest.*, 2007, **19**, 525-531.  
1520
- 1521 9 J. R. Ingelfinger, *N. Engl. J. Med.*, 2008, **26**, 2745-2748.  
1522
- 1523 10 S. A. Tittlemier, *Food Addit. Contam.*, 2010, **27**, 129-145.  
1524
- 1525 11 Y. N. Wu and Y. Zhang, *Food Chem. Toxicol.*, 2013, **56**, 325-335.  
1526
- 1527 12 W. Chansuvarn, S. Panich and A. Imyim, *Spectrochim. Acta Part A*, 2013, **113**, 154-158.

- 1528
- 1529 13 G. Venkatasami and J. R. Sowa Jr., *Anal. Chim. Acta*, 2010, **665**, 227-230.
- 1530
- 1531 14 H. W. Sun, L. X. Wang, L. F. Ai, S. X. Liang and H. Wu, *Food Control*, 2010, **21**, 686-691.
- 1532
- 1533 15 S. Goscinny, V. Hanot, J-F. Halbardier, J-Y. Michelet, J. Van Loco, *Food Control*, 2011, **22**,
- 1534 226-230.
- 1535
- 1536 16 X. Xia, S. Y. Ding, X. W. Li, X. Gong, S. X. Zhang, H. Y. Jiang, J. C. Li and J. Z. Shen, *Anal.*
- 1537 *Chim. Acta*, 2009, **651**, 196-200.
- 1538
- 1539 17 X. L. Zhu, S. H. Wang, Q. Liu, Q. Xu, S. X. Xu and H. L. Chen, *J. Agric. Food Chem.*, 2009,
- 1540 **57**, 11075-11080.
- 1541
- 1542 18 B. R. Shang, Y. Q. Chen, Z. Y. Wang, W. J. Yang and L. Y. Zhang, *J. Anim. Vet. Adv.*, 2001, **1**,
- 1543 73-80.
- 1544
- 1545 19 X. M. Xu, Y. P. Ren, Y. Zhu, Z. X. Cai, J. L. Han, B. F. Huang and Y. Zhu, *Anal. Chim. Acta*,
- 1546 2009, **650**, 39-43.
- 1547
- 1548 20 Y. Liu, E. E. D. Todd, Q. Zhang, J. R. Shi and X. J. Liu, *Univ-Sci B (Biomed & Biotechnol)*,
- 1549 2012, **13**, 525-532.
- 1550
- 1551 21 F. X. Sun, W. Ma, L. G. Xu, Y. Y. Zhu, L. Q. Liu, C. F. Peng, L. B. Wang, H. Kuang and C. L.
- 1552 Xu, *Trac-Trend Anal. Chem.*, 2010, **29**, 1239-1249.
- 1553
- 1554 22 Y. C. Tyan, M. H. Yang, S. B. Jong, C. K. Wang and J. Shiea, *Anal. Bioanal. Chem.*, 2009, **395**,
- 1555 729-735.
- 1556
- 1557 23 D. R. Thevenot, K. Toth, R. A. Durst and G. S. Wilson, *Biosens. Bioelectron.*, 2001, **16**,

- 1558 121-131.
- 1559
- 1560 24 J. H. Kim, S. C. Mun, H. N. Ko, G. Y. Yun, and J. H. Kim, *Nanotechnology*, 2014, **25**, 1-7.
- 1561
- 1562 25 J. Janata, *Anal. Chem.*, 2001, **73**, 151-153.
- 1563
- 1564 26 M. Frost and M. E. Meyerhoff, *Anal. Chem.*, 2006, **78**, 7370-7377.
- 1565
- 1566 27 J. Janata, *Anal. Chem.*, 1990, **62**, 33-44.
- 1567
- 1568 28 M. S. Luchansky and R. C. Bailey, *Anal. Chem.*, 2012, **84**, 793-821.
- 1569
- 1570 29 D. Vilela, M. C. Gonzalez and A. Escarpa, *Anal. Chim. Acta.*, 2012, **751**, 24-43.
- 1571
- 1572 30 K. Saha, S. S. Agasti, C. Kim, X. N. Li and V. M. Rotello, *Chem. Rev.*, 2011, **112**, 2739-2779.
- 1573
- 1574 31 W. A. Zhao, M. A. Brook and Y. F. Li, *Chembiochem.*, 2008, **9**, 2363-2371.
- 1575
- 1576 32 D. B. Liu, Z. Wang and X. Y. Jiang, *Nanoscale*, 2011, **3**, 1421-1433.
- 1577
- 1578 33 K. C. Grabar, R. G. Freeman, M. B. Hommer and M. J. Natan. *Anal. Chem.*, 1995, **67**, 735-743.
- 1579
- 1580 34 L. Li, B. X. Li, D. Cheng and L. H. Mao, *Food Chem.*, 2010, **122**, 895-900.
- 1581
- 1582 35 Q. Q. Zhou, N. Liu, Z. W. Qie, Y. Wang, B. A. Ning and Z. X. Gao, *J. Agric. Food Chem.*, 2011,
- 1583 **59**, 12006-12011.
- 1584
- 1585 36 L. Q. Guo, J. H. Zhong, J. M. Wu, F. F. Fu, G. N. Chen, X. Y. Zheng and S. Lin, *Talanta*, 2010,
- 1586 **82**, 1654-1658.
- 1587

- 1588 37 H. Chi, B. H. Liu, G. J. Guan, Z. P. Zhang and M. Y. Han, *Analyst*, 2010, **135**, 1070-1075.  
1589
- 1590 38 P. J. Ni, H. C. Dai, Y. L. Wang, Y. J. Sun, Y. Shi, J. T. Hu and Z. Li, *Biosens. Bioelectron.*, 2014,  
1591 **60**, 286-291.  
1592
- 1593 39 K. L. Ai, Y. L. Liu and L. H. Lu, *J. Am. Chem. Soc.*, 2009, **131**, 9496-9497.  
1594
- 1595 40 H. C. Su, H. Fan, S. Y. Ai, N. Wu, H. M. Fan, P. C. Bian and J. C. Liu, *Talanta*, 2011, **85**  
1596 1338-1343.  
1597
- 1598 41 H. Kuang, W. Chen, W. J. Yan, L. G. Xu, Y. Y. Zhu, L. Q. Liu, H. Q. Chu, C. F. Peng, L. B.  
1599 Wang, H. Q. Chu, C. F. Peng, L. B. Wang and N. A. Kotov, *Biosens. Bioelectron.*, 2011, **26**,  
1600 2032-2037.  
1601
- 1602 42 X. S. Liang, H. P. Wei, Z. Q. Cui, J. Y. Deng, Z. P. Zhang, X. Y. You and X. E. Zhang, *Analyst*,  
1603 2011, **136**, 179-183.  
1604
- 1605 43 B. Roy, A. Saha and A. K. Nandi, *Analyst*, 2011, **136**, 67-70.  
1606
- 1607 44 R. K. Bera and C. R. Raj, *Analyst*, 2011, **136**, 1644-1648.  
1608
- 1609 45 H. A. Guan, J. Yu and D. F. Chi, *Food Control*, 2013, **32**, 35-41.  
1610
- 1611 46 Q. Cao, H. Zhao, Y. J. He, X. J. Li, L. X. Zeng, N. Ding, J. A. Wang, J. Yang and G. W. Wang,  
1612 *Biosens. Bioelectron.*, 2010, **25**, 2680-2685.  
1613
- 1614 47 Z. J. Wu, H. Zhao, Y. Xue, Q. A. Cao, J. Yang, Y. J. He, X. J. Li and Z. B. Yuan, *Biosens.*  
1615 *Bioelectron.*, 2011, **26**, 2574-2578.  
1616
- 1617 48 X. F. Zhang, Z. J. Wu, Y. Xue, Y. Zhang, H. Zhao, Y. J. He, X. J. Li and Z. B. Yuan, *Anal.*

- 1618 *Methods*, 2013, **5**, 1930-1934.
- 1619
- 1620 49 J. Li, W. Li, W. B. Qiang, X. Wang, H. Li and D. K. Xu, *Anal. Chim. Acta.*, 2014, **807**,
- 1621 120-125.
- 1622
- 1623 50 Y. R. Ma, H. Y. Niu, X. L. Zhang and Y. Q. Cai, *Analyst*, 2011, **136**, 4192-4196.
- 1624
- 1625 51 C. P. Han and H. B. Li, *Analyst*, 2010, **135**, 583-588.
- 1626
- 1627 52 H. Ping, M. W. Zhang, H. K. Li, S. G. Li, Q. S. Chen, C. Y. Sun and T. H. Zhang, *Food Control*,
- 1628 2012, **23**, 191-197.
- 1629
- 1630 53 W. W. Zhong, *Anal. Bioanal. Chem.*, 2009, **394**, 47-59.
- 1631
- 1632 54 G. W. Chen, F. L. Song, X. Q. Xiong and X. J. Peng, *Ind. Eng. Chem. Res.*, 2013, **52**,
- 1633 11228-11245.
- 1634
- 1635 55 J. Ling and C. Z. Huang, *Anal. Methods*, 2010, **2**, 1439-1447.
- 1636
- 1637 56 L. Q. Guo, J. H. Zhong, J. M. Wu, F. F. Fu, G. N. Chen, Y. X. Chen, X. Y. Zheng and S. Lin,
- 1638 *Analyst*, 2011, **136**, 1659-1663.
- 1639
- 1640 57 X. Y. Cao, F. Shen, M. W. Zhang, J. J. Guo, Y. L. Luo, J. Y. Xu, Y. Li and C. Y. Sun, *Dyes*
- 1641 *Pigments*, 2014, **111**, 99-107.
- 1642
- 1643 58 R. Gill, M. Zayats and I. Willner, *Angew. Chem. Int. Ed.*, 2008, **47**, 7602-7625.
- 1644
- 1645 59 M. W. Zhang, H. Ping, X. Y. Cao, H. K. Li, F. R. Guan, C. Y. Sun and J. B. Liu, *Food Addit.*
- 1646 *Contam.*, 2012, **29**, 333-344.
- 1647



- 1648 60 G. L. Wang, H. J. Jiao, X. Y. Zhu, Y. M. Dong and Z. J. Li, *Talanta*, 2012, **93**, 398-403.  
1649
- 1650 61 X. F. Li, J. Li, H. Y. Kuang, L. Feng, S. J. Yi, X. D. Xia, H. W. Huang, Y. Chen, C. R. Tang and  
1651 Y. L. Zeng, *Anal. Chim. Acta*, 2013, **802**, 82-88.  
1652
- 1653 62 H. Zhang, Z. Zhou, B. Yang and M. Y. Gao, *J Phys. Chem. B*, 2003, **107**, 8-13.  
1654
- 1655 63 B. T. Huy, M. H. Seo, X. F. Zhang and Y. I. Lee, *Biosens. Bioelectron.*, 2014, **57**, 310-316.  
1656
- 1657 64 L. L. Li, G. H. Wu, T. Hong, Z. Y. Yin and D. Sun, *Interfaces*, 2014, **6**, 2858-2864.  
1658
- 1659 65 F. Gao, Q. Q. Ye, P. Cui and L. Zhang, *J. Agric. Food Chem.*, 2012, **60**, 4550-4558.  
1660
- 1661 66 P. Yuan and D. R. Walt, *Anal. Chem.*, 1987, **59**, 2391-2394.  
1662
- 1663 67 M. W. Zhang, X. Y. Cao, H. K. Li, F. R. Guan, J. J. Guo, F. Shen, Y. L. Luo, C. Y. Sun and L. G.  
1664 Zhang, *Food Chem.*, 2012, **135**, 1894-1900.  
1665
- 1666 68 X. Y. Cao, F. Shen, M. W. Zhang, J. J. Guo, Y. L. Luo, X. Li, H. Liu, C. Y. Sun and J. B. Liu,  
1667 *Food Control*, 2013, **34**, 221-229.  
1668
- 1669 69 X. Y. Cao, F. Shen, M. W. Zhang and C. Y. Sun, *Sensor Actuat. B*, 2014, **202**, 1175-1182.  
1670
- 1671 70 L. Shang, S. J. Dong, and G. U. Nienhaus, *Nano Today*, 2011, **6**, 401-418.  
1672
- 1673 71 L. B. Zhang and E. K. Wang, *Nano Today*, 2014, **9**, 132-157.  
1674
- 1675 72 S. Han, S. Y. Zhu, Z. Y. Liu, L. Z. Hu, S. Parveen and G. B. Xu, *Biosens. Bioelectron.*, 2012, **36**,  
1676 267-270.  
1677

- 1678 73 H. C. Dai, Y. Shi, Y. L. Wang, Y. J. Sun, J. T. Hu, P. J. Ni and Z. Li, *Biosens. Bioelectron.*, 2014,  
1679 **53**, 76-81.  
1680
- 1681 74 J. P. Xie, Y. G. Zheng and J. Y. Ying, *Chem. Commun.*, 2010, **46**, 961-963.  
1682
- 1683 75 J. J. Du, S. Y. Yin, L. Jiang, B. Ma and X. D. Chen, *Chem. Commun.*, 2013, **49**, 4196-4198.  
1684
- 1685 76 M. Haase and H. Schafer, *Angew. Chem. Int. Ed.*, 2011, **50**, 5808-5829.  
1686
- 1687 77 D. E. Achatz, R. Ali and O. S. Wolfbeis, *Top. Curr. Chem.*, 2011, **300**, 29-50.  
1688
- 1689 78 H. S. Mader, P. Kele, S. M. Saleh and O. S. Wolfbeis, *Curr. Opin. Chem. Biol.*, 2010, **14**,  
1690 582-596.  
1691
- 1692 79 C. Hazra, V. N. K. B. Adusumalli and V. Mahalingam, *Appl. Mater. Interfaces*, 2014, **6**,  
1693 7833-7839.  
1694
- 1695 80 N. Li, D. Q. Liu and H. Cui, *Anal. Bioanal. Chem.*, 2014, **406**, 5561-5571.  
1696
- 1697 81 Z. Lin, H. Chen and J. M. Lin, *Analyst*, 2013, **138**, 5182-5193.  
1698
- 1699 82 J. A. Ocaña-González, M. Ramos-Payán, R. Fernández-Torres, M. V. Navarro and M. A.  
1700 Bello-López, *Talanta*, 2014, **122**, 214-222.  
1701
- 1702 83 M. L. Liu, Z. Lin and J. M. Lin, *Anal. Chim. Acta*, 2010, **670**, 1-10.  
1703
- 1704 84 D. L. Giokas, A. G. Vlessidis, G. Z. Tsogas and N. P. Evmiridis, *TrAC-Trends Anal. Chem.*,  
1705 2010, **29**, 1113-1126.  
1706
- 1707 85 Z. M. Wang, D. H. Chen, X. Gao and Z. H. Song, *J. Agric. Food Chem.*, 2009, **57**, 3464-3469.

- 1708
- 1709 86 Z. H. Song, L. Wang and S. Hou, *Anal. Bioanal. Chem.*, 2004, **378**, 529-535.
- 1710
- 1711 87 H. J. Zeng, R. Yang, Q. W. Wang, J. J. Li and L. B. Qu, *Food Chem.*, 2011, **127**, 842-846.
- 1712
- 1713 88 J. J. Zhang, M. Wu, D. H. Chen and Z. H. Song, *J. Food Compos. Anal.*, 2011, **24**, 1038-1042.
- 1714
- 1715 89 X. S. Tang, X. Y. Shi, Y. H. Tang, Z. J. Yue and Q. Q. He, *Luminescence*, 2012, **27**, 229-233.
- 1716
- 1717 90 J. L. Manzoori, M. Amjadi and J. Hassanzadeh, *Microchim. Acta*, 2011, **175**, 47-54.
- 1718
- 1719 91 K. Lee, L. K. Povlich and J. Kim, *Analyst*, 2010, **135**, 2179-2189.
- 1720
- 1721 92 C. Y. Sun and J. H. Li, Elsevier, *Advances in Planar Lipid Bilayers and Liposomes*, 2006, vol. 4,
- 1722 ch. 7, pp. 229-252.
- 1723
- 1724 93 M. A. Reppy and B. A. Pindzola, *Chem. Commun.*, 2007, **42**, 4317-4338.
- 1725
- 1726 94 D. J. Ahn and J. M. Kim, *Acc. Chem. Res.*, 2008, **41**, 805-816.
- 1727
- 1728 95 J. Lee, E. J. Jeong, J. Kim, *J. Chem. Commun.*, 2011, **47**, 358-360.
- 1729
- 1730 96 A. C. Chen and S. Chatterjee, *Chem. Soc. Rev.*, 2013, **42**, 5425-5438.
- 1731
- 1732 97 H. Zhu, S. X. Zhang, M. X. Li, Y. H. Shao and Z. W. Zhu, *Chem. Commun.*, 2010, **46**,
- 1733 2259-2261.
- 1734
- 1735 98 C. W. Liao, Y. R. Chen, J. L. Chang and J. M. Zen, *J. Agric. Food Chem.*, 2011, **59**, 9782-9787.
- 1736
- 1737 99 Q. A. Cao, H. Zhao, L. X. Zeng, J. Wang, R. Wang, X. H. Qiu and Y. J. He, *Talanta*, 2009, **80**,

- 1738 484-488.
- 1739
- 1740 100 T. K. Zhao, L. H. Liu, G. M. Li, A. L. Dang and T. H. Li, *J. Electrochem. Soc.*, 2012, **159**,
- 1741 141-145.
- 1742
- 1743 101 Q. A. Cao, H. Zhao, Y. J. He, N. Ding and J. A. Wang, *Anal. Chim. Acta*, 2010, **675**, 24-28.
- 1744
- 1745 102 A. Saha, B. Roy, A. Garai and A.K. Nandi, *Langmuir*, 2009, **25**, 8457-8461.
- 1746
- 1747 103 C. W. Liao, Y. R. Chen, J. L. Chang and J. M. Zen, *Electroanal.*, 2011, **23**, 573-576.
- 1748
- 1749 104 K. S. Prasad, G. Muthuraman and J. M. Zen, *Electrochem. Commun.*, 2008, **10**, 559-563.
- 1750
- 1751 105 J. L. Chang, K. H. Chang, C. C. Hu, W. L. Cheng and J. M. Zen, *Electrochem. Commun.*,
- 1752 2010, **12**, 596-599.
- 1753
- 1754 106 L. M. Zhang, T. Li, P. Yu, T. Ohsaka and L. Q. Mao, *Electrochem. Commun.*, 2013, **26**, 89-92.
- 1755
- 1756 107 M. M. Richter, *Chem. Rev.*, 2004, **104**, 3003-3036.
- 1757
- 1758 108 X. B. Yin, S. Dong and E. Wang, *TrAC Trends Anal. Chem.*, 2004, **23**, 432-441.
- 1759
- 1760 109 Z. Y. Guo, P. P. Gai, T. T. Hao, S. Wang, D. Y. Wei and N. Gan, *Talanta*, 2011, **83**, 1736-1741.
- 1761
- 1762 110 F. Y. Liu, X. Yang, and S. G. Sun, *Analyst*, 2011, **136**, 374-378.
- 1763
- 1764 111 Y. H. Wang, X. X. He, K. M. Wang, J. Su, Z. F. Chen and G. P. Yan, *Chem. J. Chinese U.*,
- 1765 2012, **33**, 1162-1166.
- 1766
- 1767 112 H. M. Cao, X. Q. Hu, C. Y. Hu, Y. Zhang and N. Q. Jia, *Biosens. Bioelectron.*, 2013, **41**,

- 1768 911-915.
- 1769
- 1770 113 L. M. Zhou, J. S. Huang, L. Yang, L. B. Li and T. Y. You, *Anal. Chim. Acta.*, 2014, **821**, 57-63.
- 1771
- 1772 114 S. A. Piletsky and A. P. F. Turner, *Electroanal.*, 2002, **14**, 317-323.
- 1773
- 1774 115 M. C. Blanco-López, M. J. Lobo-Castanón, A. J. Miranda-Ordieres, P. Tunón-Blanco, *Trends*
- 1775 *Anal. Chem.*, 2004, **23**, 36-48.
- 1776
- 1777 116 Liang, R. M. Zhang and W. Qin, *Sensor Actuat. B*, 2009, **141**, 544-550.
- 1778
- 1779 117 A. Pizzariello, M. Stred, S. Stred'anska, S. Miertus, *Actuators B: Chem.*, 2001, **76**, 286-294.
- 1780
- 1781 118 J. P. Li, Z. Q. Chen and Y. P. Li, *Anal Chim. Acta.*, 2011, **706**, 255-260.
- 1782
- 1783 119 P. Jin, B. Yu, S. Z. Yang and H. H. Ma, *Microchim. Acta*, 2011, **174**, 265-271.
- 1784
- 1785 120 L. özcan and Y. Sahin, *Sensor Actuat. B*, 2007, **127**, 362-369.
- 1786
- 1787 121 A. Gómez-Caballero, M.A. Goicolea, R.J. Barrio, *Analyst*, 2005, **130**, 1012-1018.
- 1788
- 1789 122 A. Gómez-Caballero, A. Ugarte, A. Sanchez-Ortega, N. Unceta, M. A. Goicolea and R. J.
- 1790 Barrio, *J. Electroanal. Chem.*, 2010, **638**, 246-253.
- 1791
- 1792 123 Y. T. Liu, J. Deng, X. L. Xiao, L. Ding, Y. L. Yuan, H. Li, X. T. Li, X. N. Yan and L. L. Wang,
- 1793 *Electrochim. Acta*, 2011, **56**, 4595-4602.
- 1794
- 1795 124 F. Xu, M. N. Gao, G. Y. Shi, L. Wang, W. Zhang, J. Xue, L. T. Jin, J. Y. Jin, *Anal. Chim. Acta*,
- 1796 2001, **439**, 239-246.
- 1797

- 1798 125 A. Benyoucef, F. Huerta, J. L. Vázquez, E. Morallon, *Eur. Polym. J.*, 2005, **41**, 843-852.  
1799
- 1800 126 K. J. Huang, C. X. Xu, W. Z. Xie, W. Wang, *Colloid. Surf. B*, 2009, **74**, 167-171.  
1801
- 1802 127 Y. Z. Zhang, J. Wang, M. L. Xu, *Colloid. Surf. B*, 2010, **75**, 179-185.  
1803
- 1804 128 B. W. Wu, Z. H. Wang, D. X. Zhao and X.Q. Lu, *Talanta*, 2012, **101**, 374-381.  
1805
- 1806 129 G. L. Xu, H. L. Zhang, M. Zhong, T. T. Zhang, X. J. Lu and X. W. Kan, *J. Electronal. Chem.*,  
1807 2014, **713**, 112-118.  
1808
- 1809 130 S. Baskar, C. W. Liao, J. L. Chang, J. M. Zen, *Electrochim. Acta*, 2012, **88**, 1-5.  
1810
- 1811 131 T. H. Tsai, S. Thiagarajan and S. M. Chen, *J. Agric. Food Chem.*, 2010, **58**, 4537-4544.  
1812
- 1813 132 Ü. T. Yilmaz and Z. Yazar, *Food Anal. Methods*, 2012, **5**, 119-125.  
1814
- 1815 133 Q. Xu, H. P. Wei, S. Du, H. B. Li, Z. P. Ji and X. Y. Hu, *J. Agric. Food Chem.*, 2013, **61**,  
1816 1810–1817.  
1817
- 1818 134 M. Farré, R. Brix and D. Barceló, *TrAC-Trends Anal. Chem.*, 2005, **6**, 532-545.  
1819
- 1820 135 S. Rodriguez-Mozaz, M-J. Lopez de Alda and D. Barceló, *Anal. Bioanal. Chem.*, 2006, **386**,  
1821 1025-1041.  
1822
- 1823 136 A. D. Ellington and J. W. Szostak, *Nature*, 1990, **346**, 818-822.  
1824
- 1825 137 M. Citartan, S. C. B. Gopinath, J Tominaga, S. C. Tan and T. H. Tang, *Biosens. Bioelectron.*,  
1826 2012, **34**, 1-11.  
1827

- 1828 138 J. W. Liu, Z. H. Cao and Y. Lu, *Chem. Rev.*, 2009, **109**, 1948-1998.  
1829
- 1830 139 S. Song, L. Wang, J. Li, J. Zhao and C. Fan, *TrAC-Trends Anal. Chem.*, 2008, **27**, 108-117.  
1831
- 1832 140 D. L. Chen, Meena, S. K. Sharma and L. W. McLaughlin, *J. Am. Chem. Soc.*, 2004, **126**,  
1833 70-71.  
1834
- 1835 141 W. J. Qi, D. Wu, J. Ling and C. Z. Huang, *Chem. Comm.*, 2010, **46**, 4893-4895.  
1836
- 1837 142 H. Huang, L. Li, G. H. Zhou, Z. H. Liu, Q. Ma, Y. Q. Feng, G. P. Zeng, P. Tinnefeldc and Z. K.  
1838 He, *Talanta*, 2011, **85**, 1013-1019.  
1839
- 1840 143 W. Yun, H. Li, S. Q. Chen, D. W. Tu, W. Y. Xie and Y. Huang, *Eur. Food Res. Technol.*, 2014,  
1841 **238**, 989-995.  
1842
- 1843 144 H. B. Xing, S. S. Zhan, Y. G., Wu, L. He and P. Zhou, *RSC Adv.*, 2013, **3**, 17424-17430.  
1844
- 1845 145 Z. G. Chen, G. L. Liu, M. H. Chen, Y. R. Peng and M. Y. Wu, *Anal. Biochem.*, 2009, **384**,  
1846 337-342.  
1847
- 1848 146 W. Cai, Y. Y. Fan, Z. L. Jiang and J. E. Yao, *Talanta*, 2010, **81**, 1810-1815.  
1849
- 1850 147 G. Q. Wen, A. H. Liang, Y. Y. Fan, Z. L. Jiang and C. N. Jiang, *Plasmonics*, 2010, **5**, 1-6.  
1851
- 1852 148 Z. L. Jiang, Y. Y. Fan, M. L. Chen, A. H. Liang, X. J. Liao, G. Q. Wen, X. C. Shen, X. C. He,  
1853 H. C. Pang and H. S. Jiang, *Anal. Chem.*, 2009, **81**, 5439-5445.  
1854
- 1855 149 A. H. Liang, L. P. Zhou and Z. L. Jiang, *Plasmonics*, 2011, **6**, 387-392.  
1856
- 1857 150 A. H. Liang, L. P. Zhou, H. M. Qin, Y. Zhang, H. X. Ouyang and Z. L. Jiang, *J. Fluoresc.*,

- 1858 2011, **21**, 1907-1912.
- 1859
- 1860 151 M. Farré, L. Kantiani and D. Bàrceló, *TrAC-Trends Anal. Chem.*, 2007, **26**, 1100-1112.
- 1861
- 1862 152 S. D. Gan and K. R. Pate, *J. Invest. Dermatol.*, 2013, **133**, 1-3.
- 1863
- 1864 153 L. Asensio, I. González, T. García, R. Martín, *Food Control*, 2008, **19**, 1-8.
- 1865
- 1866 154 H. Y. Zhang and S. Wang, *J. Immunol. Methods*, 2009, **350**, 1-13.
- 1867
- 1868 155 H. Y. Zhang, S. Wang and G. Z. Fang, *J. Immunol. Methods*, 2011, **368**, 1-23.
- 1869
- 1870 156 E. Watanabe, S. Miyake and Y. Yogo, *J. Agric. Food Chem.*, 2013, **61**, 12459-12472.
- 1871
- 1872 157 J. X. Liu, Y. B. Zhong, J. Liu, H. C. Zhang, J. Z. Xi and J. P. Wang, *Food Control*, 2010, **21**,
- 1873 1482-1487.
- 1874
- 1875 158 H. T. Lei, Y. D. Shen, L. J. Song, J. Y. Yang, O. P. Chevallier, S. A. Haughey, H. Wang, Y. M.
- 1876 Sun and C. T. Elliott, *Anal. Chim. Acta*, 2010, **665**, 84-90.
- 1877
- 1878 159 H. T. Lei, R. Su, S. A. Haughey, Q. Wang, Z. L. Xu, J. Y. Yang, Y. D. Shen, H. Wang and Y. M.
- 1879 Sun, *Molecules*, 2011, **16**, 5591-5603.
- 1880
- 1881 160 Y. Zhou, C. Y. Li, Y. S. Li, H. L. Ren, S. Y. Lu, X. L. Tian, Y. M. Hao, Y. Y. Zhang, Q. F. Shen,
- 1882 Z. S. Liu, X. M. Meng and J. H. Zhang, *Food Chem.*, 2012, **135**, 2681-2686.
- 1883
- 1884 161 B. Y. Cao, H. Yang, J. Song, H. F. Chang, S. Q. Li and A. P. Deng, *Talanta*, 2013, **116**,
- 1885 173-180.
- 1886
- 1887 162 K. Zhu, J. C. Li, Z. H. Wang, H. Y. Jiang, R. C. Beierc, F. Xu, J. Z. Shen and S. Y. Ding,



- 1888 *Biosens. Bioelectron.*, 2011, **26**, 2716-2719.
- 1889
- 1890 163 L. Trapiella-Alfonso, J. M. Costa-Fernandez, R. Pereiro and A. Sanz-Medel, *Talanta*, 2013,
- 1891 **106**, 243-248.
- 1892
- 1893 164 B. B. Dzantiev, N. A. Byzova, A. E. Urusov and A. V. Zherdev, *TrAC-Trend Anal. Chem.*,
- 1894 2014, **55**, 81-93.
- 1895
- 1896 165 X. M. Li, P. J. Luo, S. S. Tang, R. C. Beier, X. P. Wu, L. L. Yang, Y. W. Li and X. L. Xiao, *J.*
- 1897 *Agr. Food Chem.*, 2011, **59**, 6064-6070.
- 1898
- 1899 166 T. Le, P. F. Yan, J. Xu and Y. J. Hao, *Food Chem.*, 2013, **138**, 1610-1615.
- 1900
- 1901 167 Z. Z. Wang, D. J. Zhi, Y. Zhao, H. L. Zhang, X. Wang, Y. Ru and H. Y. Li, *Int. J. Nanomed.*,
- 1902 2014, 1699-1705.
- 1903
- 1904 168 Jiri Homola, *Chem. Rev.*, 2008, **108**, 462-493.
- 1905
- 1906 169 K. V. .Ragavan, N. K. Rastogi and M. S. Thakur, *TrAC-Trends Anal. Chem.*, 2013, **52**,
- 1907 248-260.
- 1908
- 1909 170 T. L. Fodey, C. S. Thompson, I. M. Traynor, S. A. Haughey, D. G. Kennedy and S. R. H.
- 1910 Crooks, *Anal. Chem.*, 2011, **83**, 5012-5016.
- 1911
- 1912 171 H. N. Wua, H. Y. Li, F. Z.H. Chu, S. Fong and Y. Li, *Sensor Actuat. B*, 2013, **178**, 541-546.
- 1913
- 1914 172 Q. Wang, S. A. Haughey, Y. M. Sun, S. A. Eremin, Z. F. Li, H. Liu, Z. L. Xu, Y. D. Shen and
- 1915 H. T. Lei, *Anal. Bioanal. Chem.*, 2011, **399**, 2275-2284.
- 1916
- 1917 173 H. L. Guo, X. H. Zhou, Y. Zhang, B. D. Song, L. H. Liu, J. X. Zhang and H. C. Shi, *Sensor*

1918 *Actuat. B*, 2014, **194**, 114-119.

1919

1920 **Figure captions**

1921 Fig.1 Novel recognition and transducer components used for the fabrication of sensors for  
1922 melamine determination.

1923

1924 Fig.2 Schematic presentation of the colorimetric mechanism for melamine determination  
1925 employing unmodified AuNPs (A) and modified AuNPs (B).

1926

1927 Fig.3 The mechanism of FRET between AuNPs and dyes for detection of melamine.

1928

1929 Fig.4 The mechanism of IFE between AgNPs and QDs for detection of melamine.

1930

1931 Fig.5 Aptamer-based colorimetric sensor for the detection of melamine.

1932

Table 1 AuNPs-based colorimetric sensing of melamine.

Analyte	Analytical Principle		Limit of Determination (LOD)	Analytical Samples	Time	Ref.
	Functionalization	Interaction				
melamine	unmodified (●)	hydrogen bonds (NH...N)	0.4 ppm	raw milk	12 min	34
melamine	unmodified (●)	hydrogen bonds (NH...N)	1 ppm	liquid milk	10 min	35
melamine	unmodified (●)	hydrogen bonds (NH...N)	0.15 ppm 2.5ppm	liquid milk infant formula	30 min	36
melamine	unmodified (●)	hydrogen bonds (NH...N)	~25 ppb	infant milk	within 5 min	37
melamine	unmodified (●)	hydrogen bonds (NH...N)	0.025 ppb	raw milk and milk powder	—	38
melamine	cyanuric acid derivative (MTT—●)	hydrogen bonds (NH...N, NH...O)	2.5 ppb	raw milk and infant formula	within 1 min	39
melamine	3-mercaptopropionate-sulfonate-modified (MPS—●)	hydrogen bonds (N...O, NH...O)	1.008 ppb	milk and infant formula	within 30 min	40
melamine	18-crown-6-thiol	hydrogen bonds (NH...O)	6 ppb	raw milk	less than 1 min	41
melamine	cysteamine	hydrogen bonds	1 ppm	milk products, eggs and feeds	—	42
melamine	riboflavin	hydrogen bonds (NH...N, NH...O)	0.1 ppm	—	—	43
melamine	2,4,6-trinitrobenzenesulfonic acid (TNBS—●)	charge-transfer	5 ppb	infant formula	within 1 min	44
melamine	uracil-5-carboxylic acid (UCA—●)	hydrogen bonds (NH...N)	0.1 ppm	—	—	—
melamine	chitosan	hydrogen bonds	6 ppb	liquid milk	20 min	45
melamine	—	hydrogen bonds (NH...O)	1 ppb	—	—	46
melamine	—	hydrogen bonds (NH...O)	0.2 ppb	liquid milk	—	47
melamine	—	hydrogen bonds (NH...O)	0.08 ppb	liquid milk	—	48

● AuNPs

Fig. 1

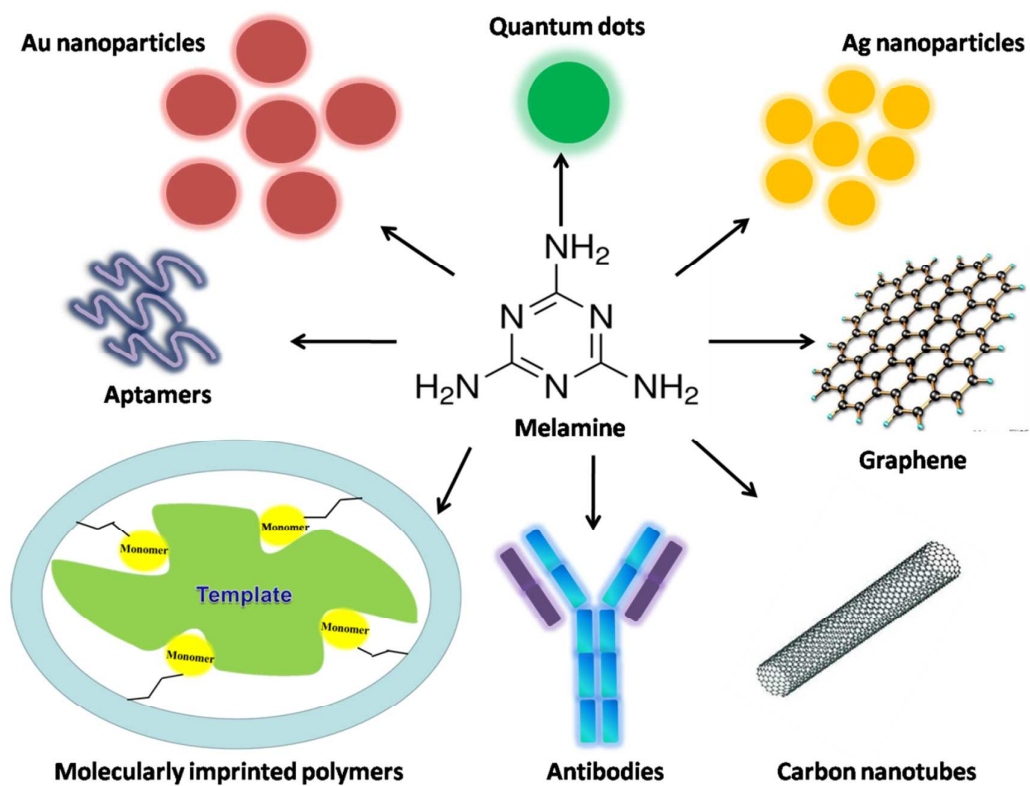


Fig. 2A

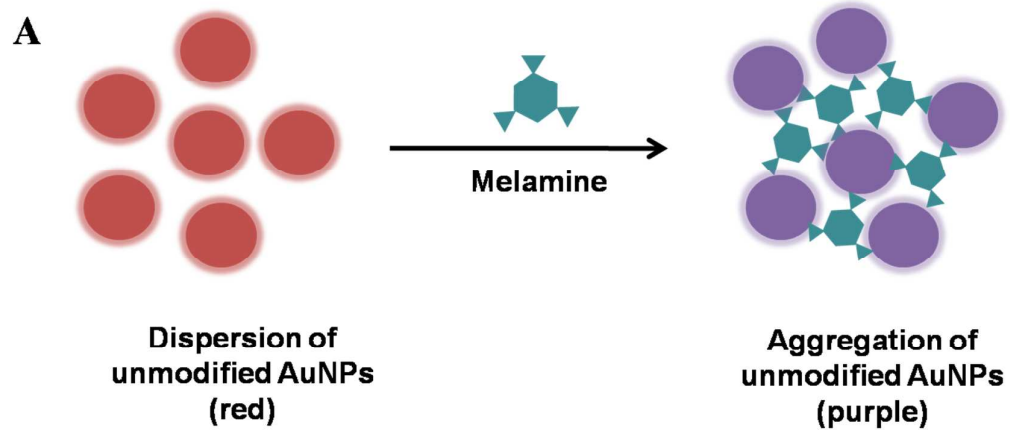


Fig. 2B

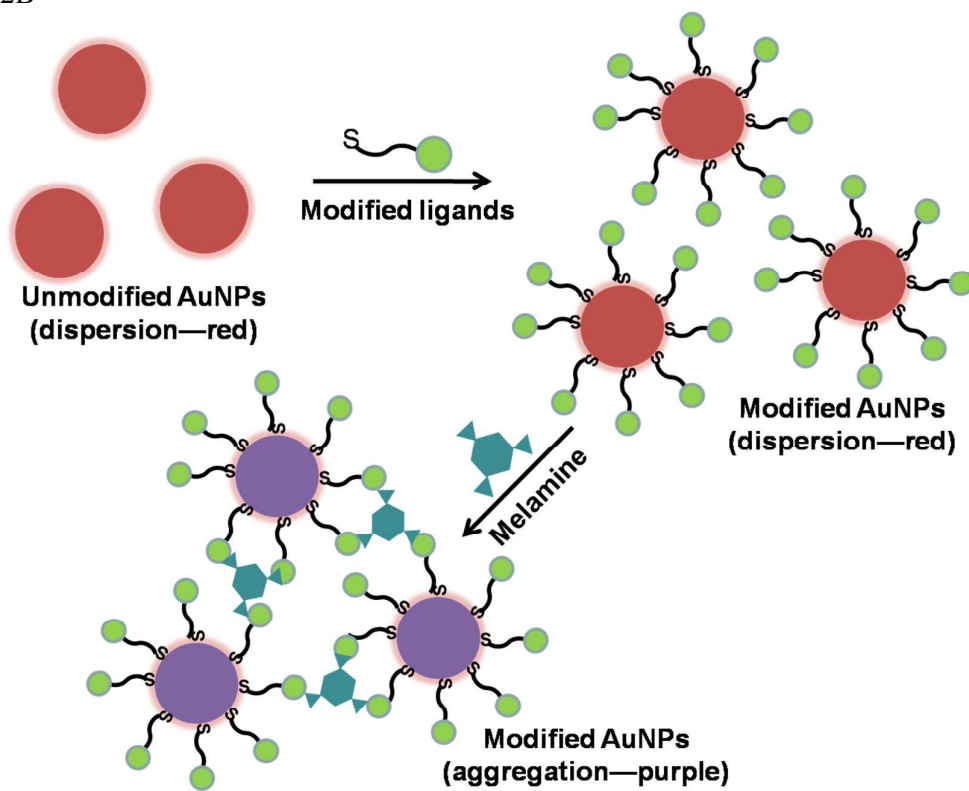
**B**

Fig. 3

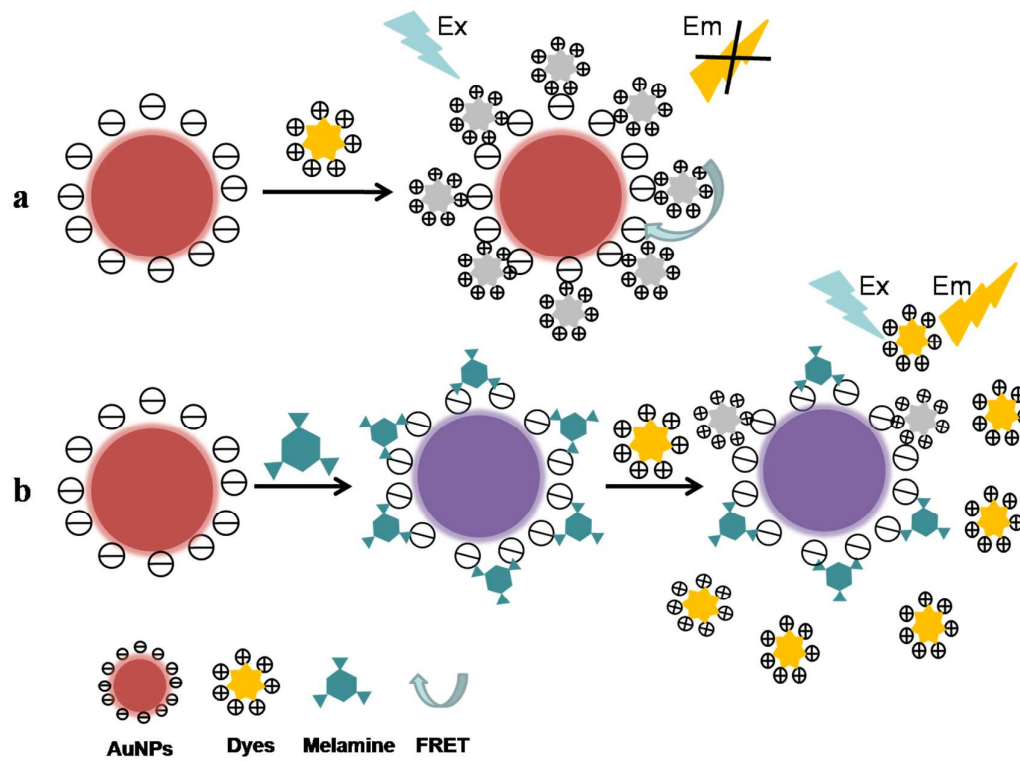


Fig. 4

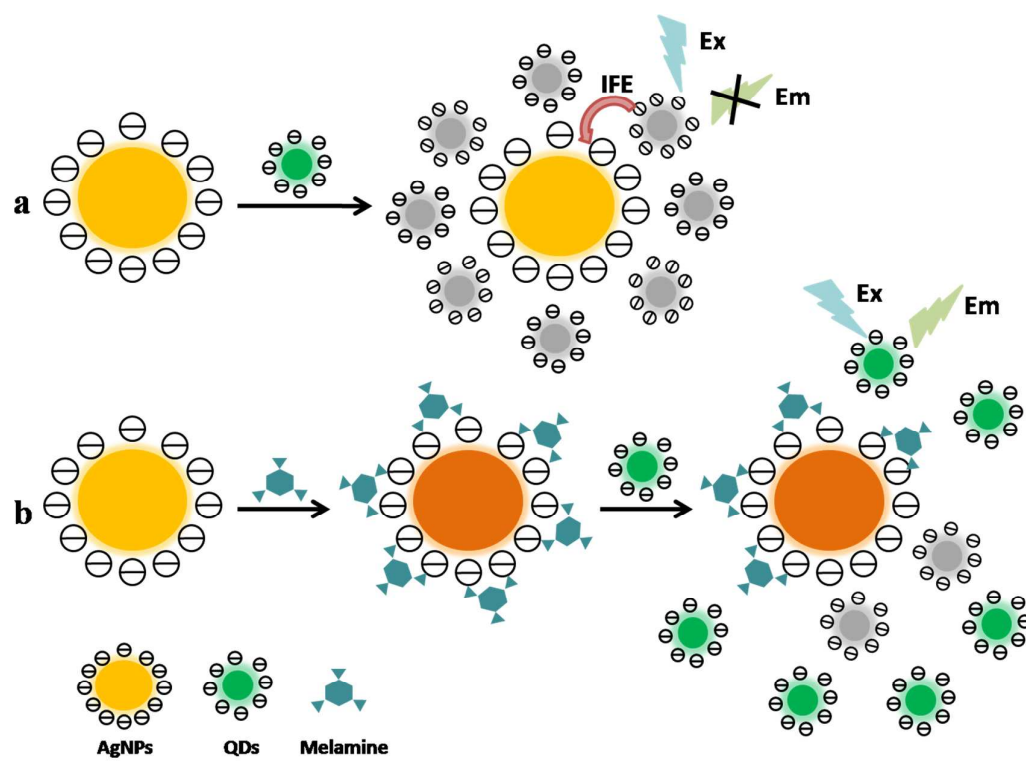




Fig. 5

